J O S H U A

THE JOURNAL OF SCIENCE AND HEALTH AT THE UNIVERSITY OF ALABAMA

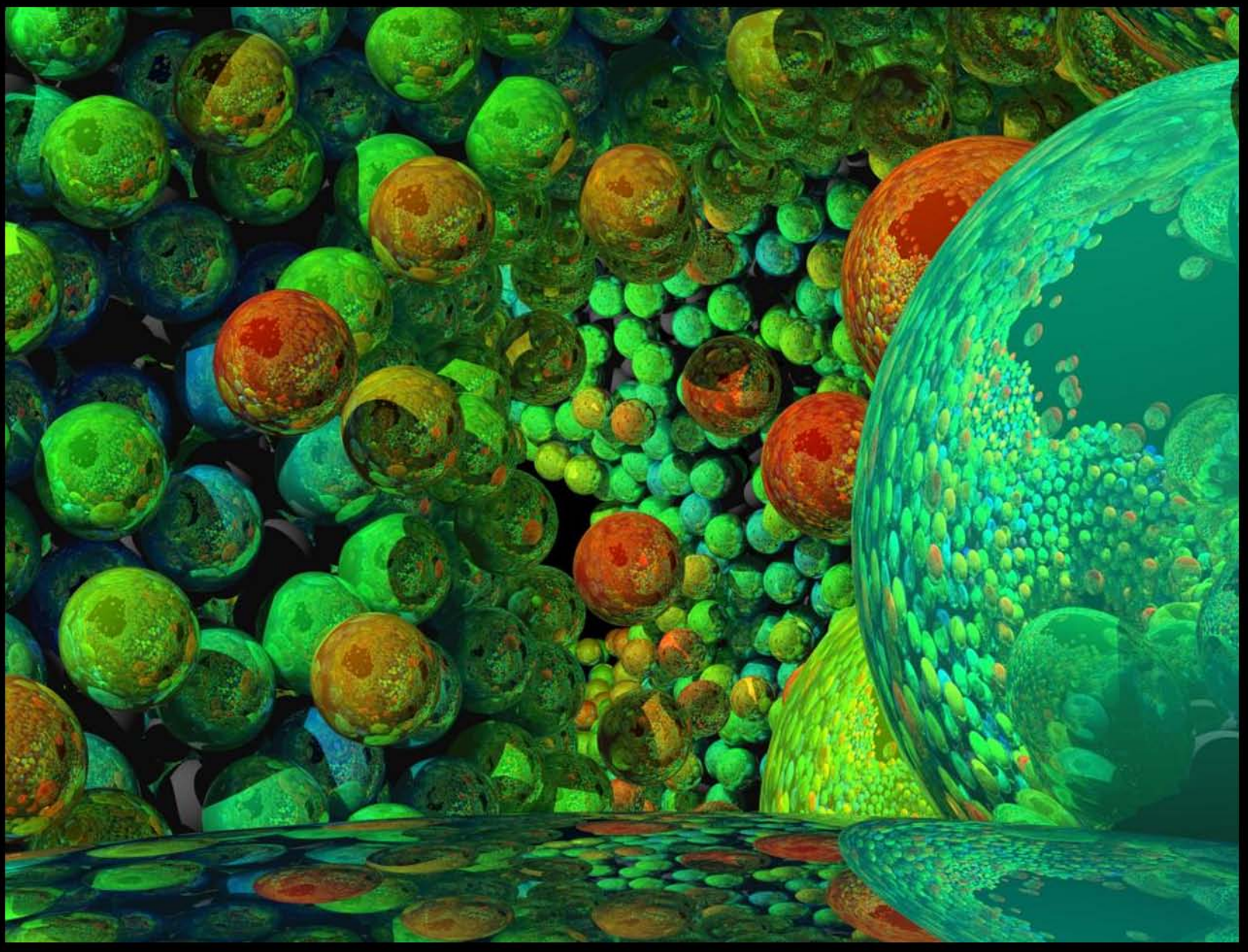

MAY 2010 VOLUME 7

JOSHUA

The University of Alabama
May 2010|Volume 7

Questions should be directed to
joshua.alabama@gmail.com

Website: bama.ua.edu/~joshua

From the Editor

Welcome!

Undergraduate research is an irreplaceable experience for any science major, providing perspective and insight beyond those found in textbooks or classrooms. In the lab, the student is able to advance the scientific frontier instead of confining his education to past results. Through presentations at symposiums, publications in prestigious journals, and forming networks with colleagues, the academic opportunities afforded by research are broad. Such experiences will prepare the student for graduate or professional school. Working in a collaborative environment, pursuing individual excellence, and communicating with confidence and efficacy are just a few of the many skills one can acquire from time in the lab.

My first undergraduate research experience was in the spring of 2007. I studied proton exchange membrane fuel cells. My concerns for the environment led me to investigate this method of producing an alternative energy source. However, besides environmental issues, I was also interested in biotechnology, resulting in me studying novel, magnetic biomaterials for targeted drug delivery, magnetic resonance imaging, and other biological applications. Since conducting undergraduate research, I have been exposed to limitless opportunities. I have presented my work all over the nation from Auburn, AL to Philadelphia, PA, and co-authored a manuscript, which was published in *IEEE Transactions on Magnetics*. Additionally, I authored an article that was published in the May 2008 edition of *JOSHUA*.

Research is ultimately what you make of it. The best and most supportive mentors I have encountered during my undergraduate years have been in the lab from professors, to graduate students, and even my fellow classmates. I have benefitted from their knowledge, patience, and advice. However, lab is more than a place where the boundaries of scientific knowledge are pushed. It is also a supportive community, filled with those with whom you can share laughter over a bit of dinner.

It is truly a privilege that I had the opportunity to serve as the 2009-2010 editor of *JOSHUA*. For many authors, this journal serves as an entry into the realm of research and scientific writing. For others, this is an opportunity to express their interests in a significant science or health topic. Join me in honoring the undergraduate researchers and authors of the May 2010, Volume 7 of *JOSHUA*.

Best Wishes,

Ynhi Thai

CONTENTS

COVER

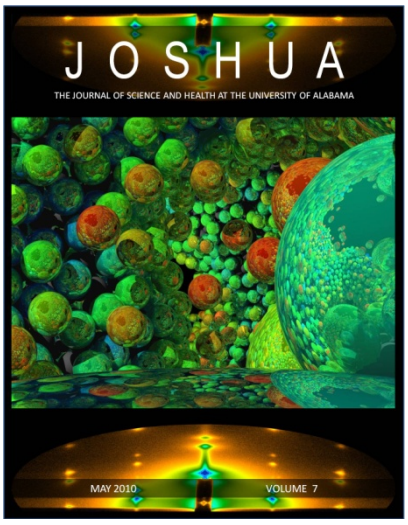

The center image depicts spherical mesoporous silica. See Allen et al. on page 3. Center graphic created and copyrighted by Dr. Lev Gelb, Washington University, St. Louis. The top and bottom images depict spots resulting from Bragg scattering of the mesoporous silica pores, created by Allen et al. Enough thanks cannot also be given to Dr. Heath Turner, The University of Alabama, Tuscaloosa, for his assistance in the design of this cover.

RESEARCH

Above:

Above:

REVIEW

Grazing Incidence Small Angle X-ray Scattering (GISAXS) Study of Mesoporous Silica Thin Films on Metal Substrates

James Allen[1], Roger Campbell, Ph.D.[2] , *Martin Bakker, Ph.D.[1] , Rainer Schad, Ph.D. [3], Dong Ryeol Lee, Ph.D.[4] , Xuefa Li, Ph.D.[4] , Jin Wang, Ph.D.[4]

*Faculty Sponsor

1. Department of Chemistry, The University of Alabama, Tuscaloosa, AL 35487, USA
2. Department of Chemistry, The University of West Alabama, Livingston, AL 35470, USA
3. Department of Physics, The University of Alabama, Tuscaloosa, AL 35487, USA
4. Advanced Photon Source, Argonne National Laboratory, Argonne, IL 60439, USA

Mesoporous silica (MS) thin films contain ordered arrays of nanometer-sized pores and are of interest for many applications. Prior work using GISAXS, a scattering/diffraction technique that allows determination of pore spacing and degree of ordering and alignment, found that for MS templated by the block co-polymer, Pluronic P123, the type of metal substrate used impacts the size, spacing, ordering, and alignment of the pores. It is expected that different block co-polymer templates will similarly impact the pore spacing, ordering and alignment in unique ways. We report here an analysis of GISAXS data from MS thin films on a range of metals templated by the block co-polymers, Pluronic P123 and Pluronic L92.

Introduction

A material is said to be mesoporous if it has pores with diameters from 2-50 nm [12]. Mesoporous materials, in general, have large surface areas, and this gives them great potential in many chemical applications [16]. One mesoporous material, in particular, that has sparked considerable interest is mesoporous silica (MS). In the early 1990's, researchers at the Mobil Research and Development Corporation developed a method called Surfactant Templating. This method was able to produce mesoporous silica in which the pores were uniform in size, evenly spaced, and well aligned with respect to each other [2]. Furthermore, the researchers found that by adjusting the template with which the MS was synthesized, it was possible to align the pores into set patterns such as hexagonal and spherical pore orientations. In the mid-90's, scientists at the University of California, Santa Barbara reported that using block co-polymers as a liquid crystal template, rather than the ionic surfactants used by the Mobil research group, allows for a wider variety of both pore shapes and sizes in MS [1]. This new method, of which SBA-15 and SBA-16 are the most common examples, became the standard for preparing MS with large pore sizes.

With the ability to both predict and manipulate the arrangement of the pores, research interest in MS expanded beyond catalysis—the original application for which the Mobil researchers had developed MS—into many different branches of nanoscience. Currently, researchers are exploring the use of MS in a broad range of applications including chromatography, fuel cells, sensors, and data storage [5,7,8,11,13,14,15].

The benefit of using a liquid crystal template, such as the block co-polymers of SBA-15, to form mesoporous silica is the wide range of surfaces upon which the silica can be formed. These surfaces are called substrates and can vary from microscope slides to silicon wafers [1,9,19]. Despite this, most research has focused on using only silica as the substrate. For many applications, however, a conductive substrate such as a metal electrode would be ideal. Studies using glass coated with indium tin oxide as a conductive substrate have been conducted, but little had been done, until recently, to explore the use of metal electrodes as substrates [10,17].

Researchers at the University of Alabama were among the first to examine the use of metal substrates in mesoporous silica thin films [3]. Their findings demonstrated that it is possible to form MS on the surfaces of nickel, tantalum, ruthenium, silver, aluminum, copper, iron, chromium, titanium, tungsten, and vanadium. This validates the use of metals as substrates. An unexpected finding was the

variation of deformation of the pore structure after the template was removed. MS on silica or silicon is known to shrink vertically after template removal [18]. Similarly, it was observed in all samples that the distance between the pores shrank perpendicularly to the substrate after template removal. This is referred to as "elongation". The research showed that the extent of elongation depended on what metal substrate was used. This unexpected variation raises many questions as to the nature of the chemical interactions between the metal substrate and the MS. It also poses the question of how the different metal substrates will affect certain treatments on MS such as metal plating.

One of the successes of nanoscience is the formation of nanometer-sized wires or nanowires. These infinitesimally small wires hold great potential in future electronics because their size allows them to bridge the gap between the electronics of classical physics and the theorized electronics of quantum physics. The applications of this technology are vast and still largely unknown but of immediate concern is how to make these tiny wires. Creating a wire that is a billionth of a meter in diameter is no trivial feat, but the use of MS as a nanowire template could greatly simplify their synthesis.

The concept is straightforward [3]. MS would be templated from block co-polymers. Once the MS hardens, the block co-polymers would then be removed, opening the pores as described above. At this point, having a conductive (i.e. metal) substrate would allow a variety of metals such as nickel to be electroplated into the pores of the MS. Because the pore size is in the range of 2-50 nm, the electroplated metal would form an array of nanowires. The MS could then be etched away, leaving the nanowires exposed for possible applications. Because the size and shape of the MS pores are determined by the specific type of block co-polymer used, a wide variety of nanowire shape and sizes could feasibly be produced. Mesoporous silica does, however, present some problems as a template, mainly ordering and domain size.

It is very rare to have a MS thin film in which all of the pores are in perfect alignment. Instead, pores will form domains in which a group of pores are aligned with each other. These domains can be large or small. As domains get larger, the thin film is said to be more ordered; the opposite is true as domains grow smaller. How well pores align in the same plane is described as orientational ordering. In many cases, most of the pores will lie in the plane of the substrate; however, more often than not, some domains will have pores which align outside of this plane. The degree to which this happens is the orientational ordering. Samples that have more pores aligned in the same plane are said to be better orientationally ordered. Naturally, films that are well ordered should be able to produce larger, ordered arrays of nanowires and are preferred to less ordered films.

The average domain size and the orientational ordering can be quantified using established techniques such as x-ray diffraction. However, the focus of this report was to study the spacing and orientation of pores in MS thin films on metal and to see how plating metal into MS affected the pores. The information gleaned in this report will further an explanation of how MS interacts with metal substrates and what effects metal plating into the MS pores might have on the pores' structure.

Methodology

The thin films were measured using a technique called Grazing Incidence Small Angle X-ray Scattering (GISAXS). GISAXS uses a high intensity x-ray to graze the surface of a thin film; the photons from the x-ray are scattered by the electrons in the atoms of the thin film. These photons are then collected by a detector, which stored the data as a picture (Figure 1). The high intensity x-ray used to collect the data was generated by a synchrotron and then filtered through a monochromator to produce x-rays of uniform wavelength. The samples were placed upon a stage that can be tilted to precisely control the angle of incidence, and the system was then evacuated via vacuum to minimize x-ray scattering from air molecules.

In regions where the pores were in a regular pattern (i.e., a domain), Bragg scattering occurs from the x-rays. Because domains have both horizontal and vertical components, Bragg scattering results in spots on GISAXS images (Figure 2). These spots can occur at different angles, depending upon how the domain is oriented with respect to the x-ray beam. If the sample has low orientational ordering, many domains will have different orientations with respect

to the x-ray beam. This causes the spots to arc along what are known as Debye-Scherrer rings (Figure 3) [4,6].

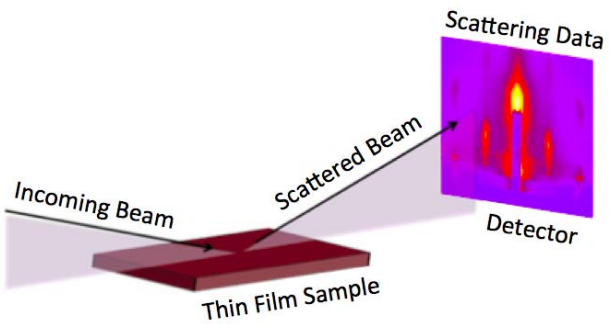

Figure 1. Diagram of GISAXS. The incoming beam represents the x-ray source and the scattering data displays an example of what the picture from the detector might look like for a typical thin film.

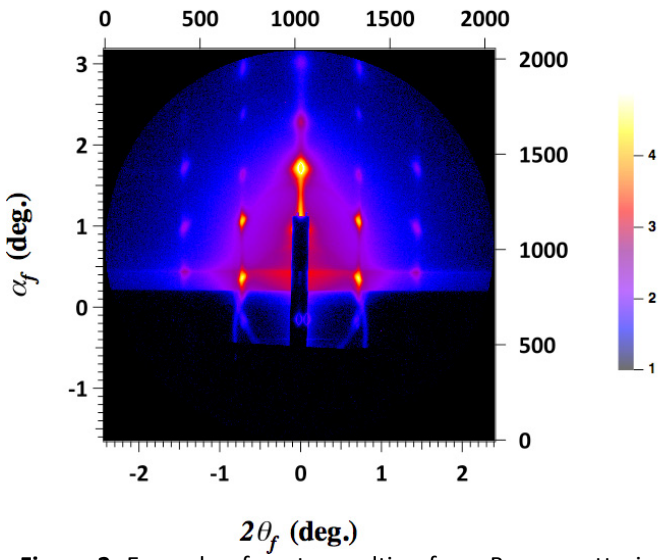

Figure 2. Example of spots resulting from Bragg scattering of MS pores.

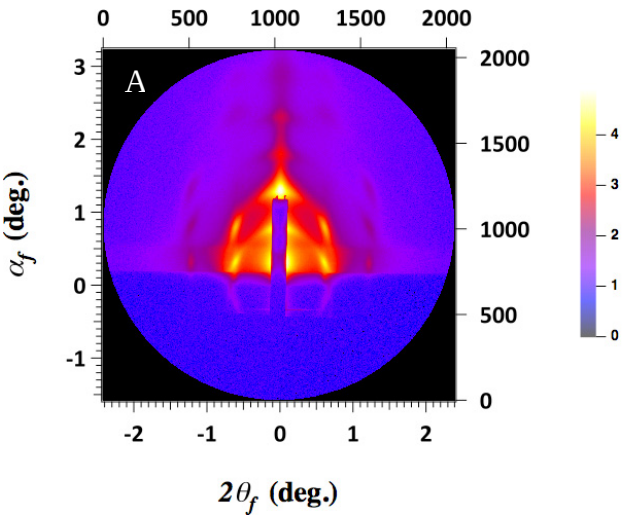

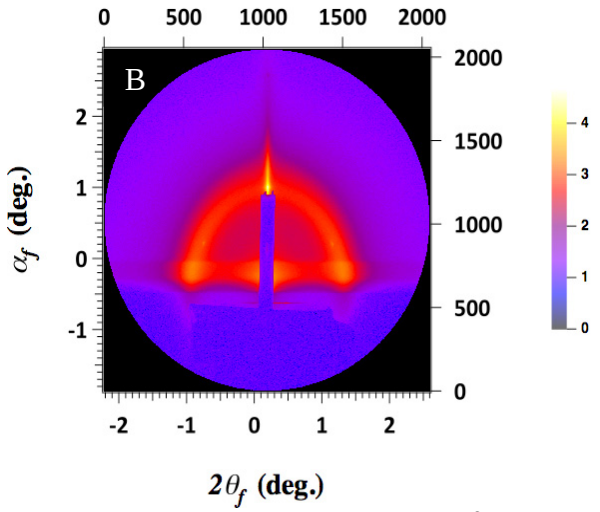

Figure 3. Figure 3a demonstrates arcing of spots along Debye-Scherrer ring due to orientational disorder. Figure 3b demonstrates Debye-Scherrer rings from high orientational disorder.

The pore spacing and orientation were determined by measuring the spacing between specific horizontal and vertical spots. These are related by Bragg's Law to the spacing between the pores, referred to as d spacing. The ratio of the horizontal and vertical d spacing can further be used to determine the orientation of the pores with respect to each other as discussed below.

Results

d Spacing

The two block co-polymers used in this study were Pluronic P123 and Pluronic L92. These are chemically similar compounds, but P123 has longer chains than L92. Thus, the pores formed by P123 templated films should be larger than those of L92. One way to check this is by comparing the d spacing of the different samples. While traditionally the d spacing is reported as a single value, here it is shown as two values corresponding to the horizontal and vertical dimensions. The purpose of this distinction will become clear in the analysis below.

In Table 1, d spacing values are reported for both L92 and P123, showing the effect that the template has on the d spacing. To highlight the effect that the metal substrates can have on the d spacing, P123 templated samples on nickel, cobalt-niobium-

zirconium alloy (abbreviated as CoNbZr), and ruthenium are additionally reported.

Table 1: d spacing values.

	Vertical d spacing	Horizontal d spacing	Vert./Hor. Ratio
P123			
Tantalum	4.93 nm	7.84 nm	0.629
Tungsten	3.77 nm	6.86 nm	0.550
Nickel	3.22 nm	6.64 nm	0.485
CoNbZr	3.49 nm	6.59 nm	0.514
L92			
Tantalum	3.66 nm	5.67 nm	0.646
Tungsten	2.44 nm	5.14 nm	0.475

Two immediate conclusions can be drawn from the d spacing data set. First, the data obtained shows a decrease in the d spacing for the tantalum and tungsten samples when templated with L92 over P123. This correlated well with the expectation that block co-polymer L92 will produce smaller pores than that of P123. Second, each of the different metals resulted in slightly different d spacing, concurring with previous research that suggested the metal substrate has an effect on the orientation of the pores [17].

A third, less obvious, conclusion can be made concerning the geometric arrangement of the pores. It is common in crystallography to classify different crystals based on their unit cell geometry, or simply the fundamental shape that the atoms or molecules of the crystal take. Mesoporous silica is not a crystal in the strictest sense. However, because it consists of domains of ordered pores, MS can be thought of as a quasi crystal. Mesoporous silica will then have a unit cell geometry that corresponds to the arrangement of pores within its domains. This geometry is determined by the nature and concentration of the template used. In the case of Pluronic P123 and L92, the geometry was a two dimensional hexagon.

As a consequence of the hexagonal structure, the ratio of the vertical to horizontal d spacings for a perfect hexagon can be calculated. Depending on how the hexagon is oriented with respect to the substrate, the ratio will either be one over the square root of three (.577) or the square root of three over one (1.73) (see Figure 4). This ratio was calculated and reported in the third column of Table 1. It is clear that

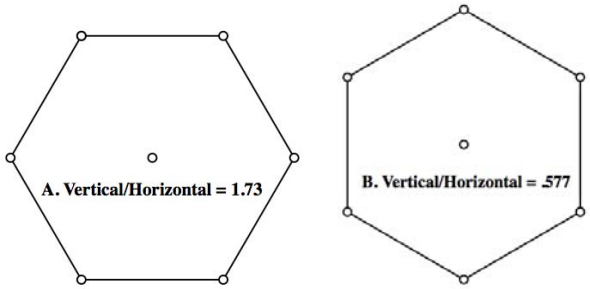

Figure 4. Images of two possible hexagonal arrangements. Pores are indicated by the hollow dots, the lines are drawn to show the hexagonal pattern.

all of the ratios were significantly closer to .577 than to 1.73, making part B of Figure 4 the likely preferred geometry of the domains.

The configuration of part A would have the largest number of pores at the substrate and air interfaces, whereas the part B configuration would result in the least number of pores at these interfaces. The hydrophobic core of the block co-polymer (what forms the pores in MS) would ideally be attracted to the air interface and be repelled by the oxides that form on the metal substrate interface. Thus, if the preferred configuration was that of part A, it would indicate that the pores were more attracted to the air interface than they were repelled by the substrate interface. This is similar for the configuration of part B. The fact that all of the metals favored B indicated that the attraction the pores have with the air interface was substantially weaker than the repulsion of the metal substrate.

Another trend of interest in Table 1 is that, with the exception of tantalum, all of the d spacing ratios were below the predicted value for a perfect hexagon of .577. This indicated that the hexagons were slightly shorter in the vertical direction—a deformation that is consistent with elongation discussed in the introduction. In this small data set, the reason for tantalum's reversal of the trend is unknown, but its consistency between L92 and P123 suggests that it is not due to chance.

Nickel Plating

Nickel was electroplated into the pores of the Pluronic P123 MS samples with the results on d spacing shown in Table 2. In the case of nickel, CoNbZr, and tungsten, the vertical to horizontal d spacing ratio increased after nickel plating. In

tantalum it decreased. The changes in tantalum and tungsten were minor and probably not significant. The increase in CoNbZr was quite significant and went well beyond the ideal ratio of .577 for a perfect hexagon. This might be due to the nickel electroplating unevenly and deforming the hexagonal structure of the MS. This theory is supported by the GISAXS images of the CoNbZr films. These films show an increase in orientational disorder after nickel was plated into the samples. This type of uneven electroplating can occur when the substrate that is being plated onto is different than the metal being plated. Such effects might also explain why the tantalum and tungsten samples did not change significantly after plating.

In the case of the nickel samples, where the substrate and plating metal are the same, the plated samples came very close to the ideal ratio of .577. From this data, it appears that filling the pores with metal after removing the template causes them to return to their original hexagonal structure, essentially reversing the effects of elongation. Because this effect was only seen in one sample, it is not sufficient to make generalizations about electroplating metal into MS pores. However, this is a promising result and suggests that metals can be plated into MS without damaging the order of the film if carried out under the right conditions. Furthermore, it might even be possible to improve the ordering of the film by electroplating metal in, as was the case with nickel.

Table 2. d spacing values before and after nickel plating.

	Vertical d spacing	Horizontal d spacing	Vert/Hor. Ratio
P123			
Tantalum	4.93 nm	7.84 nm	0.629
Tungsten	3.77 nm	6.86 nm	0.550
Nickel	3.22 nm	6.64 nm	0.485
CoNbZr	3.49 nm	6.59 nm	0.514
P123 with Nickel Plating			
Tantalum	4.72 nm	7.85 nm	0.601
Tungsten	3.87 nm	6.89 nm	0.562
Nickel	3.73 nm	6.69 nm	0.558
CoNbZr	4.83 nm	6.66 nm	0.725

Conclusion

Due to the small number of metals tested in this research, it is difficult to make any substantial conclusions regarding the chemistry between the metal substrates, templating agents, and silica of mesoporous silica. However, the data gathered confirms that this type of analysis, when applied to a larger range of substrates, will likely yield valuable insight into the impact of substrate and block co-polymer type on the quality of the mesoporous silica thin films produced.

Acknowledgments

Enough thanks cannot be given to the wonderful McNair Scholars Program at the University of Alabama for its support; the selfless staff of McNair has graciously given their time and effort to make this research possible.

References

[1] Alberius PCA, Frindell KL, Hayward RC, Kramer EJ, Stucky GD & Chmelka BF. (2002). General Predictive Syntheses of Cubic, Hexagonal, and Lamellar Silica and Titania Mesostructured Thin Films. Chem. Mater., 14:3284-3294.

[2] Beck JS, Vartuli JC, Roth WJ, Leonowicz ME, Kresge CT, Schmitt KD, Chu CTW, Olson DH, Sheppard EW, McCullen SB, Higgins JB & Schlenker J. (1992). A New Family of Mesoporous Molecular Sieves Prepared with Liquid Crystal Templates. J. Am. Chem. Soc., 114:10834-10843.

[3] Campbell R. (2008). Synthesis and Characterization of High Surface Area Three Dimensional Mesoporous Electrodes. Ph.D. Dissertation, University of Alabama, Tuscaloosa.

[4] Doshi DA, Gibaud A, Goletto V, Lu M, Gerung H, Ocko B, Han SM & Brinker CJ. (2003). Peering into the Self-Assembly of Surfactant Templated Thin-Film Silica Mesophases. J. Am. Chem. Soc., 125:11646-11655.

[5] Favier F, Walter EC, Zach MP, Benter T & Penner RM. (2001). Hydrogen Sensors and Switches from Electrodeposited Palladium Mesowire Arrays. Science, 293:2227-2231.

[6] Gibaud A, Grosso D, Smarsly B, Baptiste A, Bardeau JF, Babonneau F, Doshi DA, Chen Z, Brinker CJ & Sanchez C. (2003). Evaporation-Controlled Self-Assembly of Silica Surfactant Mesophases. J. Phys. Chem. B., 107:6114-6118.

[7] Huczko A. (2000). Template-Based Synthesis of Nanomaterials. Appl. Phys. A: Mater. Sci. Process, 70:365-376.

[8] Long JW, Dunn B, Rolison DR & White HS. (2004). Three-Dimensional Battery Architectures. Chem. Rev., 104:4463-4492.

[9] Lu Y, Ganguli R, Drewien CA, Anderson MT, Brinker CJ, Gong W, Guo Y, Soyez H, Dunn B & Huang MH. (1997). Continuous Formation of Supported Cubic and Hexagonal Mesoporous Films by Sol-Gel Dip-Coating. Nature, 389:364-368.

[10] Luo H, Wang D, He J & Lu Y. (2005). Magnetic Cobalt Nanowire Thin Films. J. Phys. Chem. B., 109:1919-1922.

[11] Metzger RM, Konovalov VV, Sun M, Xu T, Zangari G, Xu B. Benakli M & Doyle WD. (2000). Magnetic Nanowires in Hexagonally Ordered Pores of Alumina. IEEE Trans. Magn., 36:30-35.

[12] Rouquerol J, Avnir D, Fairbridge CW, Everett DH, Haynes JH, Pernicone N, Ramsay JDF, Sing KSW & Unger KK. (1994). Recommendations for the Characterization of Porous Solids. Pure Appl. Chem., 66:1739-1758.

[13] Routkevitch D, Bigioni T, Moskovits M & Xu JM. (1996). Electrochemical Fabrication of CdS Nanowire Arrays in Porous Anodic Aluminum Oxide Templates. J. Phys. Chem., 100:14037-14047.

[14] Walter EC, Penner RM, Liu H, Ng KH, Zach MP & Favier F. (2002). Sensors from Electrodeposited Metal Nanowires. Surf. Interface Anal., 34:409-412.

[15] Walter EC, Zach MP, Favier F, Murray BJ, Inazu K, Hemminger JC & Penner RM. (2003). Metal Nanowire Arrays by Electrode position. Chem. Phys. Chem., 4: 131-138.

[16] Wan Y & Zhao D. (2006). On the Controllable Soft-Templating Approach to Mesoporous Silicates. Chem. Rev., 107:2821-2860.

[17] Wang D, Zhou WL, McCaughy BF, Hampsey JE, Ji X, Jiang YB, Xu H, Tang J, Schmehl RH, O'Connor C, Brinker CJ & Lu Y. (2003). Electrodeposition of Metallic Nanowire Thin Films using Mesoporous Silica Templates. Adv. Mater., 15:130-133.

[18] Zickler GA, Jahnert S, Funari SS, Findenegg GH & Paris O. (2007). Pore Lattice Deformation in Ordered Mesoporous Silica Studied by in situ Small-Angle X-ray Diffraction. J. Appl. Crystallogr., 40:s522-s526.

[19] Zhao D, Yang P, Melosh N, Feng J, Chmelka BF & Stucky GD. (1998). Continuous Mesoporous Silica Films with Highly Ordered Large Pore Structures. Adv. Mater., 10:1380-1385.

James Allen is a senior from Hoover, Alabama, majoring in chemistry, economics, and math. He has worked in the laboratory of Dr. Martin Bakker in the Department of Chemistry since the spring of 2009 as a McNair Scholar. He is also a member of Phi Beta Kappa, a Presidential Scholar, and the William Ray Moore Memorial Physical Science Scholarship recipient.

Changes in Bacterial Communities in Coastal Plain Streams: The Influence of Beaver Wetlands

Kaylan Gee, Kirsten Ansorge, *Jennifer Edmonds, Ph.D.
*Faculty Sponsor

Department of Biological Sciences, The University of Alabama, Tuscaloosa, AL 35487, USA

Beaver dams create wetlands that are fundamentally different from other wetlands. Their geomorphic position in the landscape, short persistence at a particular location, and close association with human management make them dynamic, but understudied as a component of low-gradient stream networks in the southeastern United States. In these ecosystems, beavers create a mosaic of patches that vary in time with dam failure and conversion of the wetland back to a stream configuration. This work relates beaver dam demise in a Coastal Plain stream (Payne Creek) to bacterial community composition in benthic sediments. We used a molecular "fingerprint" analysis (T-RFLP) to test the prediction that the influence of beaver-created wetlands on sediment bacterial communities is evident as long as two decades after a wetland drained. Significant differences in samples from 3 stream reaches, collected 6 times from January-October 2009, suggest this wetland legacy is present, likely mediated through differences in organic matter abundance and bioavailability. We also found temporal changes in bacterial community composition possibly linked to shorter time frame phenomena such as leaf fall, flooding, or dramatic changes in temperature.

Introduction

A wetland is a transitional area of land where the soil is saturated with moisture, either seasonally or permanently. Wetlands, often called the "kidneys" of the environment, play a major role in environmental regulation of water and waste. If there are areas of urbanization or agriculture in the watershed, pesticides, fertilizers, and other pollutants may enter the wetland system. The pollutants are taken up into the biomass of vegetation and bacteria in the wetland. Bacteria can also chemically alter the pollutants and, in many cases, reduce their toxicity [6]. Recently, there has been a movement to protect wetlands against pollution and to prevent them from being directly destroyed by urban and agricultural development [12]. Common types of wetlands include swamps, marshes, floodplains, and bogs. Wetlands can have saltwater, freshwater, or brackish water. We examined freshwater beaver wetlands in the coastal plain physiographic province of the southeastern United States. These wetland ecosystems have been highly understudied by researchers.

Beavers are considered one of the world's few species of "ecosystem engineers," or animals that significantly alter their environment and, thus, increase biodiversity in the area. When a beaver builds a dam on a stream, a wetland develops upstream. This new wetland provides a unique habitat for various species of organisms [14]. Human impact on beaver populations through alteration or elimination of their habitat can have a major impact on the overall landscape and wetland development [1]. We focused on how the demise of beaver dams influences biodiversity and ecosystem function in relation to bacterial species. Seventeen years of observations by UA faculty in local stream networks with embedded beaver wetlands has allowed us to develop a strong conceptual framework for how ecosystem processes might change in response to beaver activity. Observations tell us that, as a wetland transitions back into a stream after the failure of a beaver dam, the sediment and organic build-up that had been concentrated around the impoundment remains in the stream, significantly impacting microbial growth in the water and sediment. The soils outside the stream that were once water-saturated drain and eventually become a beaver meadow, which is gradually reforested. This transformation creates a slow change in the intensity and character of terrestrial-aquatic linkages, particularly with regards to the bioavailability of organic matter available for decomposition in the

sediments. Therefore, the study of beaver wetlands is essential to understand how these changes influence carbon cycling in streams.

Beaver wetlands create sudden change in an ecosystem, whereas other types of wetlands have a much more gradual impact on the environment. For instance, local vegetation is significantly altered when beavers dam a part of a stream. New types of aquatic or semi-aquatic vegetation grow in place of non-aquatic species. Forests are turned into bogs as beaver dams convert them into aquatic ecosystems. After beavers abandon the area, forestation gradually returns [5]. Beaver wetlands also influence the production of greenhouse gases. Beaver dams generate conditions that are favorable for methanogenesis, leading to higher production of methane in the area. These higher levels of methane have an impact on overall methane concentrations across the northern hemisphere [10]. Our conceptual model considered beaver-created wetlands as nodes on the landscape that are extremely dynamic. Beaver ponds may be created in a week and may remain embedded in the stream network for as little as 4 years or for as long as 4 decades. Age of a beaver wetland depends on size, climatic conditions, and human interference. The transition from beaver wetland back to stream ecosystem is a frequent occurrence in the Gulf Coastal Plains, based on our personal observation, but has been relatively understudied.

Although most research relating to extant beaver wetlands is concentrated in northern North America, there have been few investigations into southeastern beaver-created wetlands. The beaver populations in the Southeast have varied significantly over the last half-century, decreasing after 1983 due to changes in trapping policies [11]. Southeastern beaver wetlands tend to be restricted to watershed areas of about 2500 hectares that show no discrimination or preference for streams crossed by roads [4]. Hydrological research in the southeast has shown that the water upstream of beaver dams tends to be of a higher pH and has higher concentrations of dissolved organic carbon (DOC) than does the water downstream of the dams [9]. DOC is a significant chemical component of wetland waters. The source of DOC is plant matter, which is produced in the aquatic ecosystem or transported by runoff coming from terrestrial soils [8]. DOC influences the removal of aquatic pollutants, particularly hydrophobic organic contaminants, like some pesticides, in one of two ways. One way is by stimulating larger populations of heterotrophic bacteria that chemically transform the pollutant during growth on the DOC. The second is by the direct absorption of the pollutant to DOC compounds. The larger the bacterial population, the more pollutants can possibly be removed from the water [6]. Levels of DOC in wetlands vary, and levels tend to fluctuate most dramatically during the summer and fall when there is more bacterial activity breaking down DOC [7].

We specifically focused on the relationship between DOC sources to coastal plain streams and the bacterial communities living in the sediments. It is believed that bacterial community structure is similar to community structure formed by macro organisms [3]. Communities of bacteria will often self-organize so that different species with similar characteristics cluster together to fill the same niche in their environment, which is known as functional redundancy. Functional redundancy in bacterial communities dampens the variability in a particular bacterial process as different species thrive under different environmental conditions, maintaining the level of each function. For example, a community of bacteria living in an area of varying temperature consists of different species of bacteria, each with a different temperature tolerance. The functions of the community such as photosynthetic activity or decomposition of DOC may be preserved even with variations in temperature levels. However, if environmental conditions (temperature, water chemistry, light levels) change dramatically, a new community structure will develop [13]. Here, we discuss our year-long investigation into the differences in bacterial diversity in wetland versus non–wetland environments in Payne Creek in the Talladega National Forest. We focused on how bacterial communities differed in stream sediments that previously were covered by wetlands, versus areas that have never been known to contain beaver wetlands.

TWE Site Description

Our study was conducted at Payne Creek in the Talladega National Forest (Figure 1). It is a

second-order Coastal Plain stream located in west-central Alabama (32.9206° N, 87.4405° W). Payne Creek is a nutrient-poor stream with low alkalinity and specific conductance. The stream length of the study was approximately 1000 meters long and composed of unconsolidated sand and silt, sometimes over 2 meters deep. Measurements of stream discharge water temperature and water chemistry have been intermittently recorded since 1990 and constantly recorded since 2001. Occasionally, excessive rainwater and runoff flood Payne Creek.

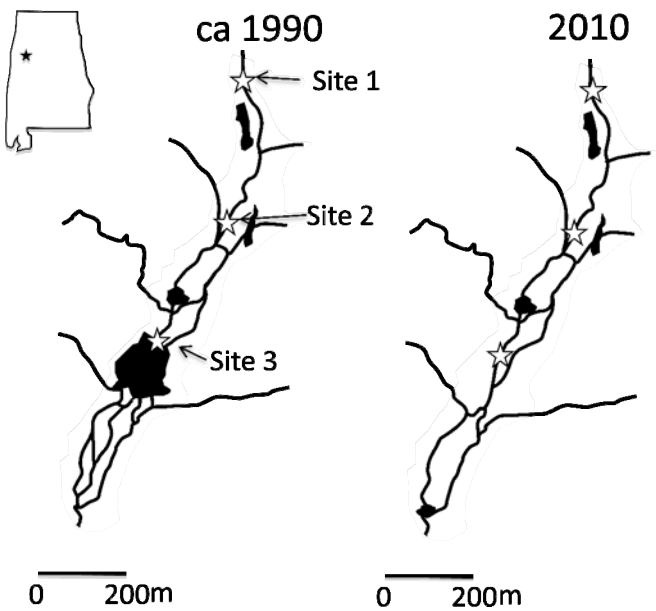

Figure 1. The star in the state of Alabama identifies the location of the Talladega National Forest. The two stream networks are Payne Creek in its current configuration versus when there was a large beaver pond and associated wetland 20 years ago. Black lines and shapes represent the ponds and streams of Payne Creek. The outlined white stars demonstrate the exact locations of sampling for this project.

Approach

We compared the bacterial communities in stream sediments, which were once a part of a large beaver wetland that drained 13 years ago. Our goal was to determine if the legacy of this wetland could be found in the composition and function of the bacterial community. An experimental design known as "space for time substitution" was used to infer the influence of the wetland. By knowing the location (or space) of the wetland in the past, sediment samples from inside and outside of its former location could be compared. This allowed identification of the differences in bacterial community composition that might be due to the wetland's previous existence.

The bacterial gene chosen for comparison was the 16S rRNA gene. This gene codes for the smaller subunit of the ribosome, which is necessary for protein creation, and is a well-known phylogenic marker used for identifying bacterial species. We performed a terminal restriction fragment length polymorphism (T-RFLP) analysis to generate a community "fingerprint" for each sample. Then, we statistically evaluated these fingerprints to look for the legacy of beaver wetlands in the stream sediments.

Methods

Continuous (15 minutes intervals) monitoring of water stage and temperature was completed using a Model 107 T probe in association with a Campbell Scientific Inc. data logger (Logan, UT) permanently mounted in the field. Stage-discharge relationships were established by making instantaneous measurements of discharge using a flow meter and channel width and depth measurements. Sediments were sampled at each site to a depth of 2 centimeters after removing the top 0.2 centimeters of sediment that would be the lighted benthic sediment. A sterile syringe was used, and sediment samples were stored in a cryovial and flash frozen at -70° C in the field. Once back in the lab, they were stored at -80° C. Water samples were taken in acid washed polypropylene containers, stored on ice until returning to the laboratory, and then filtered through a pre-combusted Whatman GF/F filter with a nominal pore size of 0.7 microns. DOC was measured on a Shimadzu 5000 TOC analyzer; nitrate, phosphate, and ammonium were measured on a Lachett autoanalyzer using standard colorimetric methods.

DNA was extracted from 1-5 grams of frozen soil using MoBio soil DNA extraction kits. Extracted nucleic acids were precipitated and resuspended in the final kit solution containing ethylenediaminetetraacetic acid (EDTA). The extracts were then stored at -20° C. Bacterial 16S rRNA genes were amplified with the primers 27F (5′-AGAGTTTGATCMTGGCTCAG-3′) and 1492Reverse (5′-AAGGAGGTGATCCANCCRCA-3′) [2]. These primers

are meant for use with microorganisms with the Bacteria domain. The forward primer was labeled with the fluorescent molecule, fluorescein (FAM). All PCR amplifications were carried out with Ready-To-Go PCR beads. Each PCR had a total reaction volume of 25 μL, with 3 μL of DNA template. Final concentrations of FAM-27F and 1492Reverse were 400 nM. Thermal cycling conditions for this amplification were as follows: (1) 3 minutes at 95° C; (2) 30 cycles of 30 seconds at 95°C, 45 seconds at 56° C, and 30 seconds at 72° C; (3) an additional elongation step at 72° C for three minutes.

Gel electrophoresis was used to confirm the 16S rRNA amplicon at a length of approximately 1500 base pairs. After confirming the amplicon, it was purified from a fluorescently-stained 1% agarose gel using a Qiagen gel extraction kit. Restriction enzyme digestion of the PCR product was carried out with the enzyme HaeIII, using the manufacturer's recommended instructions. This step cuts each PCR amplicon at a specific location and creates fragments of different sizes, depending on the 16S rRNA gene sequence of each species amplified. Digested samples were further purified by ethanol precipitation and resuspended in 12 μL of deionized formamide. One μL of DNA fragment length standard Gene-Scan-500 TAMRA (tetramethylrhodamine) was added to the sample, and all samples were denatured at 95° C. The terminal restriction fragment lengths were separated by capillary electrophoresis on an ABI Prism 310 genetic analyser. Fragments were quantified using GENESCAN analysis software, and each fragment appears as a peak on the electropherogram (Supplementary Figure S1).

Fragments smaller than 50 base pairs were excluded from the analysis in order to avoid the detection of primers. The T-RFLP data were analyzed using a Visual Basic program that reconciled minor shifts in fragment length between successive electropherograms. Peaks of less than 3% of total electropherogram area were not considered in the analysis. The relative abundance of fragments within samples was determined by calculating the area under each peak as a percentage of the total area. The fragment lengths present in each sample and the percent contribution to the total community were used to characterize the individual bacterial communities. Since particular peaks in this analysis may represent more than one bacterial taxon, the number of peaks was not considered an indication of species richness. Rather, the peaks were used for comparative purposes.

Sample fingerprints were compared using the software package PRIMER 5 (Plymouth Marine Laboratory, Plymouth, UK). To assess differences in community compositions, we used a nonparametric analysis of similarity (ANOSIM). We generated one Bray-Curtis similarity matrix using the fragment composition of the bacterial communities. This matrix was characterized in two ways, based upon sample location (Site 1, 2, or 3) or sampling date (February, March, April, May, July, or October). Differences among these groups were visualized using nonmetric multidimensional scaling (MDS) plots of the similarity matrix to produce a two-dimensional ordination figure. ANOSIM was used to test whether there were significant differences in bacterial community composition between sample sites and dates.

Results and Discussion

During 2009, we sampled on six different dates from three sites and generated T-RFLPs for each sample (Table 1). Site 1 was located farthest upstream where no beaver dam had been known to exist. This site contained sandy soil that was frequently removed and then replenished due to flooding. Site 2 was between sites 1 and 3 and may have previously been a small beaver wetland, as indicated by the vegetation structure when our collaborators first started sampling there. Site 3 was the farthest downstream, where it is known to have been a large beaver wetland that was intensively studied by UA researchers from 1990-1996. Fragment lengths found in the T-RFLP data ranged from 51–328 base pairs for all the samples, and the number of fragments per sample ranged from 8–15 fragments. Bray-Curtis similarity values were graphically represented in a 2 dimensional MDS (Figures 2 and 3). The stress value was interpreted as the difficulty in representing the difference between all the samples in graphing space, with a 3-dimensional representation usually being more accurate (lower stress) than a 2-dimensional graph. Although our stress value was higher than desired, we maintained

Table 1. Number of replicate samples at each site for each sampling date.

Sampling Date	Site 1	Site 2	Site 3	Total
23 February 2009	4	2	2	8
23 March 2009	1	2	2	5
27 April 2009	1	1	1	3
28 May 2009	1	-	2	3
28 July 2009	2	-	2	4
22 October 2009	3	-	4	7

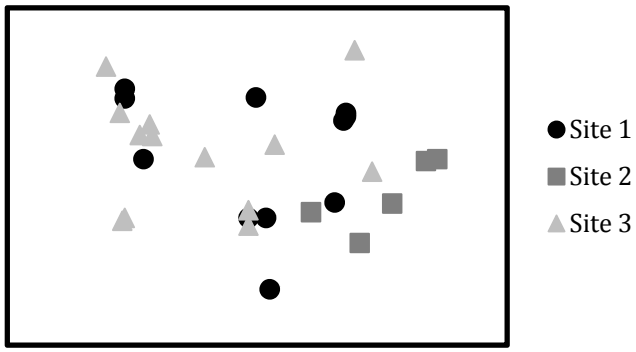

Figure 2. MDS of Bray-Curtis similarity values, based on sampling site, generated using T-RFLP data from soil samples collected in 2009.

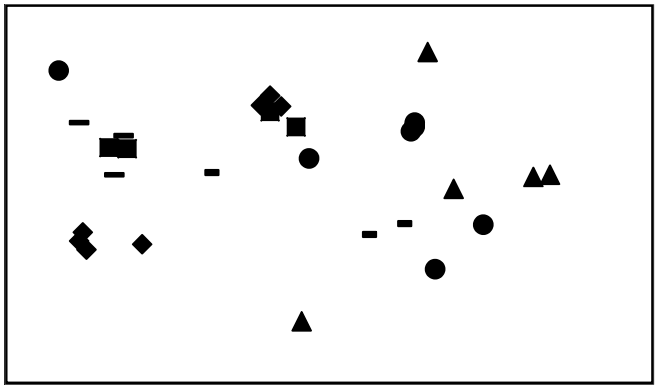

February	●	**May**	—
March	▲	**July**	■
April	-	**October**	●

Figure 3. MDS of Bray-Curtis similarity values, based on sampling date, generated using T-RFLP data from soil samples collected in 2009.

the 2-dimensional graphs for simplicity of presentation. ANOSIM analysis of the Bray-Curtis matrix showed significant differences in bacterial community diversity between 2 of the 3 sampling sites when grouping across all dates. There was a strong significant difference between sites 1 and 3, with a significance level of 0.001 (Table 2). Sites 1 and 2 were also significantly different at a level of 0.022. Sites 2 and 3 were not statistically different from each other. The samples collected in February and October (regardless of site) also varied significantly from the samples collected in other months. The significance level of February versus March, April, July, and August ranged from 0.002-0.022. The difference between February and May was not significant, but only 3 samples were analyzed from May, which makes our statistical power low. The significance level between October and the other months ranged from 0.05 to 0.017, indicating a significant difference in community composition in October compared to all other sampling dates (Table 2).

Table 2. Statistical output from two-way crossed ANOSIM.

	R Statistic	Significance Level
Global test (by site)	0.975	0.001
Pairwise Test (by site)		
Site 1 vs. Site 2	1.0	0.022
Site 1 vs. Site 3	1.0	0.001
Site 2 vs. Site 3	0.75	0.111*
Global test (by date)	0.953	0.001
Pairwise tests (by date, only significant tests reported)		
Feb vs. Mar	1.0	0.022
Feb vs. April	1.0	0.022
Feb vs. May	1.0	0.067*
Feb vs. Jul	1.0	0.022
Feb vs. Oct	1.0	0.002
Oct vs. Mar	1.0	0.017
Oct vs. April	1.0	0.05
Oct vs. May	1.0	0.017
Oct vs. Jul	1.0	0.007

* Test not significant but data are reported for completeness of comparisons.

The significant difference between sites 2 and 3, as compared to the site at the top of the reach, supported our prediction that the beaver wetland left a legacy that could be quantified based on bacterial diversity. Water chemistry data indicated that site 3 contained approximately twice as much DOC as site 1. This suggests that the presence of a beaver wetland impacts the amount and type of organic matter in an area, resulting in larger pools of organic carbon, nitrogen, and phosphorus associated with the sediments. Site 1 had never been known to contain a beaver wetland and had lower levels of stream water DOC. Site 2 had DOC levels between those of sites 1 and 3, indicating the possibility that it may have once been a beaver wetland. Also, when researchers first began studying Payne Creek in 1973, they noticed alder vegetation at site 2, which was also indicative of a past beaver wetland.

We detected differences in community structure throughout the year, indicating that changes in environmental conditions may be influencing bacterial community dynamics. The difference between samples in February and those in other months was likely due to lower temperatures (Supplementary Table S1). Low temperatures possibly selected for species in the sediments that are adapted to colder temperatures, as the total number of fragments in the February samples were not different than the number found in other months. The differences found in October may have been created by an increase in fallen leaves or due to a recent large flood (Supplementary Table S1). The average discharge of Payne Creek in October was 3-15 times higher than any other sampling date. More organic matter was passing through Payne Creek during this time, much of which originated from the soils the runoff recently passed through. The DOC in the stream in October would likely have been of a different quality or bioavailability than that found during base flow periods, whether it came from freshly fallen leaves or floodwaters, stimulating different bacterial communities to grow. There is also a possibility that the reworking of the sediments during the flood prior to our October sampling brought new bacterial species, or that bacteria derived from soil water were a greater portion of the community due to the recent flood. We will be completing a large-scale sequencing effort to further evaluate changes in community structure and the functional gene capabilities of these bacterial communities in light of the results presented here.

Conclusion

Based on our findings, we conclude that the presence of a beaver wetland leaves a lasting impact on the function and composition of bacterial communities in coastal plain stream ecosystems even after the wetland has drained. In the future, we will generate additional T-RFLPs for the various sites and dates to create a more robust and even data set. Sediment samples will continue to be collected from the sites to see if temporal patterns in bacterial communities we found in 2009 are consistent across years. The aim of this study is to understand differences in the way that carbon, nitrogen, and phosphorous are cycled through the ecosystem as a result of changes in the composition of bacterial communities.

References

[1] Butler D & Malanson G. (2005). The geomorphic influences of beaver dams and failures of beaver dams. Geomorphology, 71:48-60.

[2] Edmonds JW. (2009). Microbial Community Response to Seawater Amendment in Low-Salinity Tidal Sediments. Microbial Ecology, 58:558-568.

[3] Horner-Devine MC & Bohanna BJM. (2006). Phylogenetic clustering and Overdispersion in Bacterial Communities. Ecology, 87:S100-S108.

[4] Jakes AF, Snodgrass JW & Burger J. (2007). Castor Canadensis (Beaver) Impoundment Association with Geomorphology of Southeastern Streams. Southeastern Naturalist, 6:271-282.

[5] Johnston CA & Naiman RJ. (1990). The use of geographic information system to analyze long term landscape alteration by beaver. Landscape Ecology, 4:5-19.

[6] Luo J, Ma M, Liu C, Zha J & Wang Z. (2009). Impacts of particulate organic carbon and dissolved organic carbon on removal of polycyclic aromatic hydrocarbons, organochlorine pesticides, and

nonylphenols in a wetland. Journal of Soils and Sediments, 9:180-187.

[7] Mann C & Wetzel R. (1995). Dissolved organic carbon and its utilization in a riverine wetland ecosystem. Biogeochemistry, 31:99-120.

[8] Mann C & Wetzel R. (1996). Loading and utilization of dissolved organic carbon from emergent macrophytes. Aquatic Botany, 53:61-72.

[9] Margolis B, Castro M & Raesly R. (2001). The impact of beaver impoundments on the water chemistry of two Appalachian streams. Canadian Journal of Fisheries and Aquatic Sciences, 58:2271-2283

[10] Naiman RJ, Manning T & Johnston CA. (1991). Beaver population fluctuations and tropospheric methane emissions in boreal wetlands. Biogeochemistry, 12:1-15.

[11] Snodgrass JW. (1997).Temporal and spatial dynamics of beaver-created patches as influenced by management practices in a south-eastern North American landscape. Journal of Applied Ecology, 34: 1043-1056.

[12] Tockner K & Stanford J. (2002). Riverine Flood Plains: present state and future trends. Environmental Conservation, 29:308-330.

[13] Ward DM. (2006). Microbial diversity in natural environments: focusing on fundamental questions. Antonie van Leeuwenhoek, 90:309-324.

Kaylan Gee is a sophomore from Irmo, South Carolina, majoring in microbiology and Spanish with minors in Computer-Based Honors and the Blount Undergraduate Initiative. She conducted her research for this paper in the lab of Dr. Jennifer Edmonds on microbial ecology. She has been honored as the recipient of a Computer-Based Honors Fellowship. Kaylan is the Vice President of Administration for her sorority, Kappa Alpha Theta, a Save First volunteer, and a Justice on the SGA Judicial Board.

Kirsten Ansorge is a sophomore from Hoover, Alabama, majoring in microbiology with minors in Computer-Based Honors and chemistry. She conducted her research for this paper with Dr. Jennifer Edmonds. She also works with Dr. Matthew Jenny of the Department of Biological Sciences using similar DNA analysis methods. Kirsten is a National Merit Finalist, Presidential Scholar, and a member of the Honors Program Student Association.

Synthesis of Iron Oxide Nanoparticles with Biological Coatings

David Dozier, Soubantika Palchoudhury, *Yuping Bao, Ph.D.
*Faculty Sponsor

Department of Chemical and Biological Engineering, The University of Alabama, Tuscaloosa, AL 35487, USA

For biological and biomedical applications, it is required to produce nanoparticles that are water soluble and biocompatible. Here, we report the synthesis of iron oxide nanoparticles coated with biological molecules (e.g., gluconic acid, lactobionic acid, or polyacrylic acid) via a co-precipitation method. These nanoparticles have narrow size distribution and are highly water soluble. Because of the biological coatings, they will have great potential in numerous biomedical applications such as tissue engineering.

Introduction

Magnetic nanoparticles have shown great potential in many biological and biomedical applications such as targeted drug delivery, magnetic fluid hyperthermia, magnetic resonance imaging, and tissue engineering [1, 3, 5, 6]. All these applications require magnetic nanoparticles to be water soluble and biocompatible.

For biological and biomedical applications, magnetic iron oxide nanoparticles are the primary choice because of their biocompatibility and chemical stability. Many synthesis methods have been explored for magnetic iron oxide nanoparticles. These include organic solvent heating method, polyol method, and co-precipitation method [2, 4, 7]. The co-precipitation method is the most effective technique for preparing aqueous dispersions of iron oxide nanoparticles because the synthesis is conducted in water. For this report, we studied several biological molecules as surface coatings to achieve biocompatibility such as gluconic acid (GA), lactobionic acid (LBA), and polyacrylic acid (PAA). These molecules were used to control the particle size, to prevent the nanoparticles from aggregation, and to achieve biocompatibility.

Experimental

Synthesis

Iron oxide nanoparticles were synthesized by a modified co-precipitation method. Ferric chloride ($FeCl_3$, 0.074 g) and ferrous chloride ($FeCl_2$, 0.190 g) at a ratio of 2 to 1 were dissolved in 20 mL deionized water, which was then stirred and heated to 60 °C. The solution was bubbled with Argon gas to prevent unwanted oxidation. Subsequently, 10 mL of 2.5 M NaOH solution was injected at 60 °C and the reaction continued at that temperature for 20 minutes before the flask was removed from heating and stirring. The nanoparticles were then removed from solution by magnetic separation. During synthesis, the concentration and amount of NaOH was varied to control the particle size. A schematic drawing of the reaction set-up is shown in Figure 1.

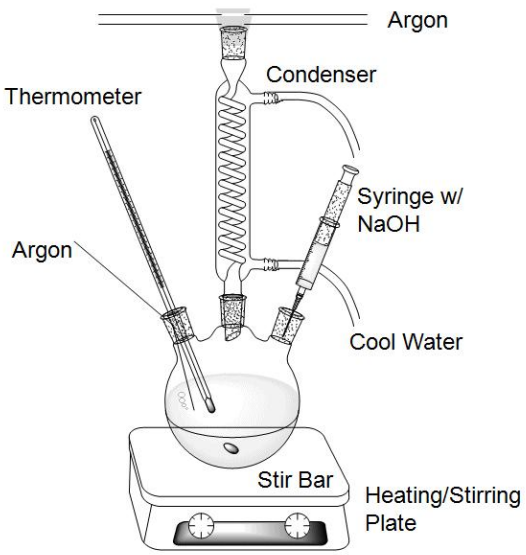

Figure 1. Schematic drawing of the experimental set-up.

Surface coatings

After synthesis, the black precipitates were collected, washed with DI water, and then re-dispersed into 10 mL GA, LBA, or PAA solutions (100 mM) under sonication. The pH was adjusted to 8 in order to simulate a biological environment and facilitate surfactant attachment to the iron oxide nanoparticles. Three hours of sonication were required to obtain well dispersed nanoparticles. The

nanoparticle solutions were then left at room temperature.

Characterization

The size and morphology of nanoparticles were studied by transmission electron microscopy (TEM); the crystal structure was verified using x-ray diffraction (XRD); the hydrodynamic size of the nanoparticles in solution was studied using dynamic light scattering (DLS). The solutions were also checked for precipitation. Solutions with a high level of precipitate indicated aggregation of nanoparticles. These aggregates are not suitable for biological applications.

Results and Discussion

Figure 2 shows the representative TEM images of iron oxide nanoparticles coated with GA and LBA. Although the sizes of both types were roughly 10 nm, the GA coated nanoparticles were more dispersed than the LBA coated nanoparticles, which showed a certain degree of aggregation.

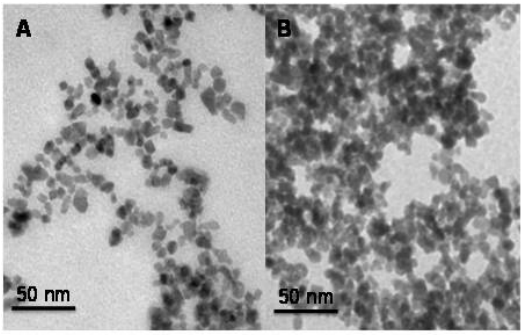

Figure 2. TEM images of iron oxide nanoparticles coated with (A) GA and (B) LBA.

The TEM image was not produced for the PAA coated iron oxide nanoparticles due to the large amount of the polymers present on the TEM grid, which interfered with the electron beam. However, the nanoparticle solution was well dispersed with no evident precipitate. Normally, precipitation is an indication of aggregation of nanoparticles.

The crystal structures of these nanoparticles were studied on GA coated nanoparticles. It was confirmed that these iron oxide nanoparticles are maghemite (Fe_2O_3), as shown in Figure 3, instead of the commonly formed magnetite nanoparticles (Fe_3O_4). This study suggests that the nanoparticles were fully oxidized either during or after the synthesis.

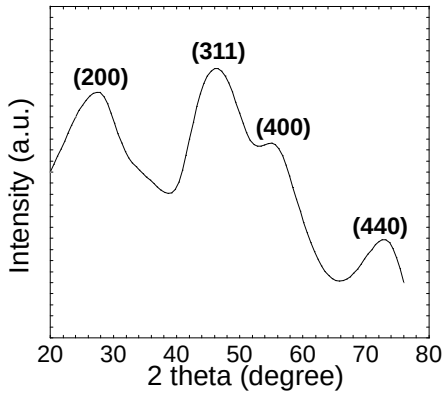

Figure 3. XRD scan of iron oxide nanoparticles.

For biological applications, nanoparticles are normally used in solution form. Therefore, it is important to study their hydrodynamic size in solution. DLS was used to measure the size of the synthesized nanoparticles. GA produced the smallest particles, showing a peak around 90 nm. LBA and PAA both had peaks around 140 nm as shown in Figure 4. The hydrodynamic sizes of the synthesized nanoparticles were significantly larger than those indicated by their TEM images. This is possibly due to the hydrogen bond formation between the carboxyl groups on adjacent surfaces, which can cause cross-linking between particles and result in a large hydrodynamic size. The size from DLS did not reveal a large difference between the MNPs synthesized with 2.5 M NaOH and 5 M NaOH.

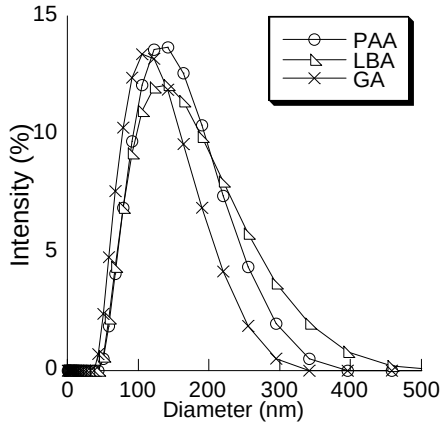

Figure 4. DLS plots of iron oxide nanoparticles coated with GA (cross), LBA (triangle), and PAA (circle).

Conclusion

In conclusion, water soluble iron oxide nanoparticles were synthesized using a co-precipitation method. These nanoparticles were subsequently coated with GA, LBA, or PAA. Both GA and LBA coatings produced well dispersed nanoparticles. They were in fully oxidized oxide form as confirmed by XRD. In solution, these nanoparticles showed a much larger hydrodynamic size, possibly due to hydrogen bond formation.

References

[1] Babes L, Denizot B, Tanguy G, Le Jeune JJ & Jallet P. (1999). Synthesis of iron oxide nanoparticles used as MRI contrast agents: A parametric study. Journal of Colloid and Interface Science, 212(2):474-482.

[2] Ge JP, Hu YX, Biasini M, Dong CL, Guo JH, Beyermann WP & Yin YD. (2007). One-step synthesis of highly water-soluble magnetite colloidal nanocrystals. Chemistry-a European Journal, 13(25):7153-7161.

[3] Gu FX, Karnik R, Wang AZ, Alexis F, Levy-Nissenbaum E, Hong S, Langer RS & Farokhzad OC. (2007). Targeted nanoparticles for cancer therapy. Nano Today, 2(3):14-21.

[4] Hyeon T. Chemical synthesis of magnetic nanoparticles. (2002). Chemical Commun., 8:927-934.

[5] Shimizu K, Ito A, Arinobe M, Murase Y, Iwata Y, Narita Y, Kagami H, Ueda M & Honda H. (2007). Effective cell-seeding technqiue using magnetite nanoparticles and magnetic force onto decellularized blood vessels for vascular tissue engineering. J. of Bioscience and Bioenginer., 103(5):472-478.

[6] Thiesen B & Jordan A. (2008). Clinical applications of magnetic nanoparticles for hyperthermia. International J. Hyperthermia, 24(6):467-474.

[7] Wenguang Y. Tonglai Z, Jianguo Z, Jinyu G & Ruifeng W. (2007). The preparation methods of magnetite nanoparticles and their morphology. Progress in Chemistry, 19(6):884-892.

David Dozier is a junior from Thomasville, Alabama, majoring in chemical engineering with a minor in biology. He currently works in the laboratory of Dr. Yuping Bao in the Department of Chemical and Biological Engineering. David also has an interest in going to medical school after graduation. He is a Presidential Scholar and a member of the Golden Key Honor Society.

Noise Mitigation by Manipulating Combustion using Porous Inert Media

L. Justin Williams, *Ajay K. Agrawal, Ph.D.
*Faculty Sponsor

Department of Mechanical Engineering, University of Alabama, Tuscaloosa, AL 35487, USA

Hearing loss from noise induced by machines, engines, and flow systems is a major concern in industry. In gas turbine engines, a major source of direct noise is the turbulent heat release process in the combustor. In this study, the combustion process is manipulated passively using high-strength, oxidation-resistant porous inert materials (PIM) rings located within the reaction zone. Effectiveness of this approach is demonstrated from noise measurements acquired in a swirl-stabilized combustor replicating typical features of a gas turbine combustor. Atmospheric pressure experiments using methane fuel were conducted for a fixed air flow rate and equivalence ratios of 0.7 and 0.8. Several PIM configurations were investigated by varying the number of PIM rings, pore density or pores per cm, and PIM ring inner diameter. Results show that the PIM geometry has a significant effect on combustion noise. Diffuser shaped ring configuration of high pore density PIM was most effective in reducing the combustion noise.

Introduction

Noise-induced hearing loss is uncommon in the home or office, but it is a major concern in industry. Accessories such as ear-plugs and noise cancelling head phones are often mandatory in certain areas; however, anyone can be negligent to these devices. Typically, sound absorbing materials are placed in the workspace to protect from the noise generated by machines, engines, flow systems, turbines, etc. While this approach minimizes the adverse effects of the noise already created, an alternative approach is to mitigate the generation of the noise itself by improving the system design. In this study, this approach was implemented to reduce combustion generated noise in systems replicating gas turbine engines. The combustion process is manipulated passively using porous inert materials (PIM), designed to resist oxidation at temperatures above 1800 K, while retaining structural strength needed to sustain the reactions.

Sound consists of pressure waves propagating through a medium, and it is quantified by the sound pressure level (SPL) measured in decibels or dB [1]. The human auditory canal concentrates pressure waves. Then small, rigid structures, called hair cells, convert the sound energy into electrical signals recorded by the brain. Long duration exposure to SPL's of 100 dB or greater can be permanently damaging to hair cells. Single bursts of 140 dB or greater can temporarily damage hair cells [1]. Mechanical devices and support structures are also subject to noise-induced fatigue, particularly when resonance occurs; structures can unexpectedly collapse, causing catastrophic failure [2].

The focus of this study was on the gas turbine engine, which is the most popular method for powering not only aircrafts, but also plants that supply electricity to homes and factories. Many sources contribute to the noise in a gas turbine engine. Examples include noise created by airflow through guide vanes, mechanical noise, jet noise, and combustion noise. Although the relative importance of each noise source varies, the combustion noise alone can be significant in many cases. The combustion noise itself is composed of direct and indirect noise. Direct combustion noise is generated by pressure fluctuations resulting from the unsteady heat release process in the turbulent flow of the reactants [4]. Indirect combustion noise is produced as the imperfectly mixed combustion products flow through the downstream components such as turbine blades. Our focus, direct combustion noise, is often the primary source of combustion noise.

Figure 1 illustrates the flow structure in a swirl-stabilized combustor, typically used in gas turbines. Reactants enter the combustor through an annular swirler. The resulting annular jet undergoes sudden expansion in the combustor, where an outer recirculation zone (ORZ) and an inner recirculation zone (IRZ) are formed on either side of the jet. These

recirculation zones trap hot products, which ignite fresh reactants in the annular jet to sustain the combustion process. The swirling motion imparted to the annular jet also helps to stabilize the flame. While recirculation zones supply the ignition energy necessary to sustain combustion, they also create vortical structures with a wide range of length and time scales. The turbulent fluctuations of vortical structures are a major source of combustion noise [5]. Thus, a method to ignite and stabilize the flame without the turbulent vortical structures can be effective in reducing the combustion noise.

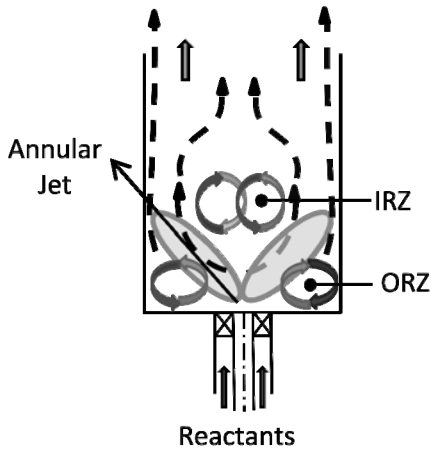

Figure 1. Flow field in a swirl stabilized combustor.

In this study, a PIM ring was placed inside the combustor as illustrated in Figure 2. The resistance to the flow caused by the PIM ring is hypothesized to intensify the swirling jet and constrain it to the core region. The PIM is also expected to eliminate the ORZ (and associated vortical structures) and to reduce the size of the IRZ [3]. Finally, a more uniform flow field is likely to emerge downstream of the PIM.

The photograph in Figure 2 shows the quartz combustor with two stacked PIM rings. The porous material is made of silicon-carbide coated carbon foam, and it offers high structural strength as well as oxidation resistance in the combustion environment. The PIM has porosity of about 0.85, i.e., the solid matrix occupies only about 15% of the flow area. The flow resistance of the PIM is affected by the pore density given in pores per cm or ppcm. Porous rings can be stacked to form different PIM configurations illustrated in Figure 3. The flow area decreases in the

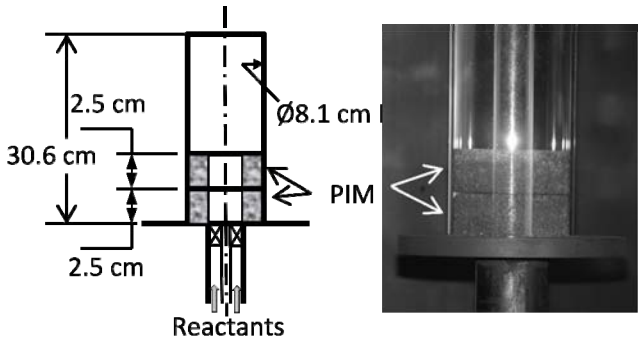

Figure 2. Placement of porous inert materials (PIM) in the combustor.

flow direction in a nozzle and increases in a diffuser configuration.

The flow area first decreases and then increases in the hyperbolic configuration, and it increases and then decreases in the elliptic configuration. In this study, only discrete changes in the flow area were considered since PIM rings of only fixed diameters were available. The objective of this study was to characterize combustion noise with and without the PIM placed inside the combustor. Experiments were conducted to understand how PIM geometry (configuration and pore density) affects combustion noise, so that an optimum PIM geometry with the minimum noise could be identified.

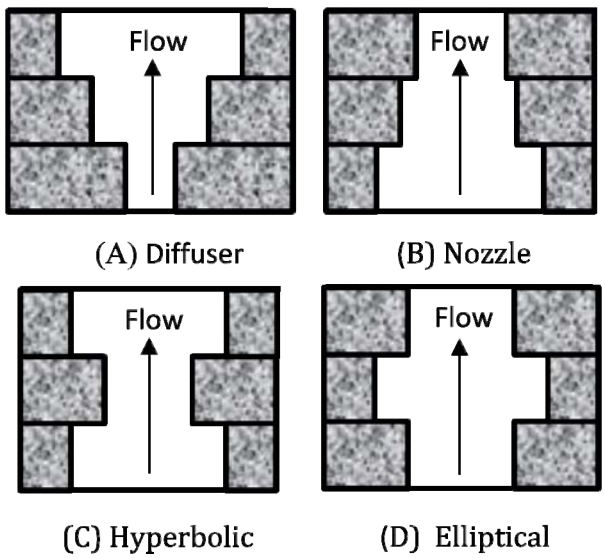

Figure 3. PIM configurations.

Experimental Setup

Figure 4 shows a schematic diagram of the experimental setup with a quartz combustor located downstream of the swirl injector. Combustion air supplied from a compressed storage tank was heated by an electrical heater, and then supplied to the mixing chamber through a plenum section to break down the turbulent flow structures. Gaseous methane from a storage tank was injected into the mixing chamber, where methane and air mixed to form homogeneous reactants at the inlet of the swirl injector. The inner and outer diameters of the swirl injector were 1.79 cm and 4.14 cm, respectively. Reactants were discharged into 8.1 cm ID, 30 cm long quart tube to complete the combustion. The combustion products from the quartz tube discharged into the ambient through a laboratory chimney and exhaust hood.

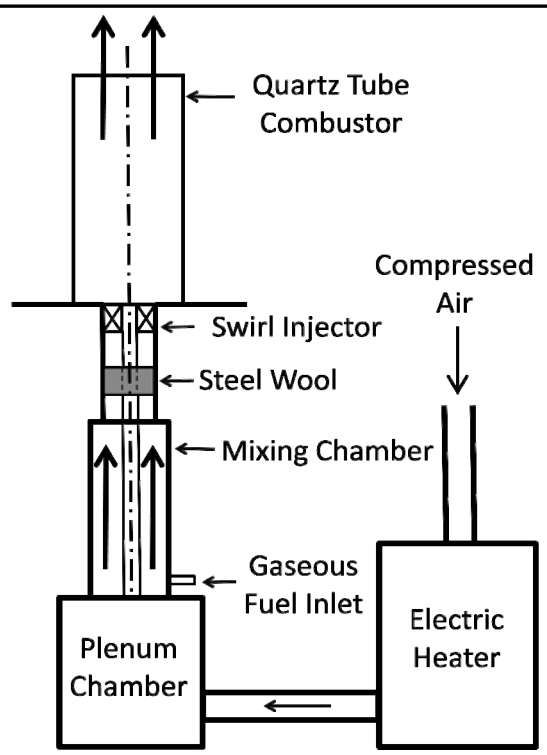

Figure 4. Experimental setup.

Calibrated laminar flow elements were used to measure the mass flow rates of air and fuel. A condenser microphone probe (BK type 4189) was used to acquire the sound measurements. The microphone probe converted pressure fluctuations into a voltage signal, which was amplified and recorded in digital form using a LabView based data acquisition system. The voltage data were acquired at 2000 Hz for 5 seconds. A fast Fourier transform algorithm was used to obtain the power spectra, expressed in terms of SPL in dB versus frequency using microphone probe calibration. The total SPL overall recorded frequencies was also computed in dB and dBA.

Experiments were conducted for fixed air flow rate of 300 standard liters per minute (SLPM) and heater exit temperature of 150°C, or combustor inlet temperature of 100˚C. The fuel flow rate was varied to obtain equivalence ratio (Ø) of 0.7 and 0.8. The PIM thickness and outer diameter were kept constant, respectively, at 2.5 cm and 8.1 cm. Experiments were conducted for different PIM configurations, formed by varying the number of PIM rings, pore density (measured in pores per cm or ppcm), and PIM inner diameter (ID). Either 2 or 3 PIM rings with pore density of 4, 8, and 18 ppcm and ID of 3.8, 4.4 or 5.1 cm were used. A nomenclature was developed to describe each configuration. For example, d38p4-d51p8-d51p18 represents a stack of three PIM rings. The first layer consists of a 3.8 cm ID PIM rings of 4 ppcm, the second layer consists of 8 ppcm PIM ring with 5.1 cm ID, and the third layer consists of 14 ppcm PIM ring with 5.1 cm ID. The sequence from left to right corresponds to the flow direction. A baseline combustor with no PIM and twenty different configurations with PIM were examined, each at Ø = 0.7 and 0.8.

Results and Discussion

Figure 5 shows photographs of the flame for the baseline combustor. The blue region in the image represents reaction zones, typically at the interfaces of the annular jet and recirculation zones. The flame structure changed in the presence of the PIM ring as shown by the photographs in Figures 6(a) and 6(b). Specifically, two modes of combustion were observed, depending upon the operating conditions. In the surface combustion mode (Figure 6a), small blue flamelets were formed at the downstream surface of the PIM, while an intense swirl-stabilized flame was established in the core region. In the interior or submerged combustion mode (Figure 6b), an intense flame in the core region was still present, but combustion also occurred inside the PIM as

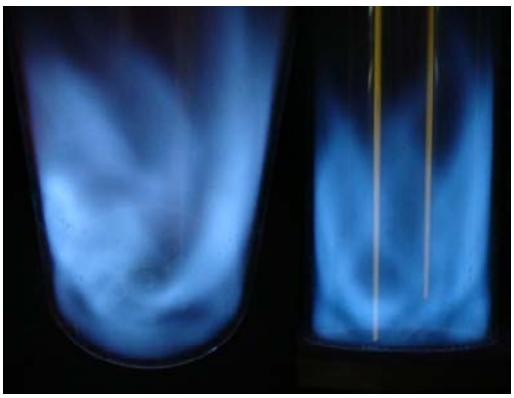

Figure 5. Baseline swirl-stabilized flame.

indicated by the intense glow. Thermal radiation from the PIM can raise combustor surface temperatures to unacceptably high levels and, hence, the interior combustion mode was deemed impractical. Measurements also indicated that the interior combustion mode increased the total SPLs.

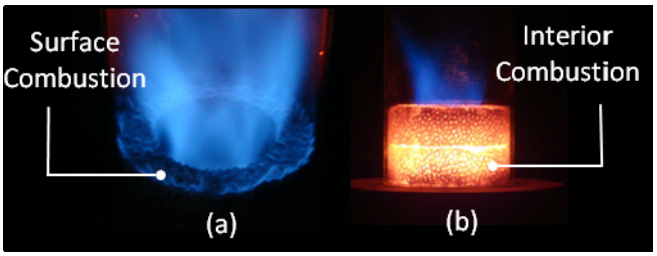

Figure 6. Swirl-stabilized flame with PIM (a) surface combustion, (b) interior combustion.

Effect of PIM Configuration

Experiments were conducted using 18 ppcm PIM ring in different configurations. Table 1 summarizes the test results in terms of the total SPL for Ø=0.7 and 0.8. The baseline combustor with no PIM (Case 1) produced total SPL of 95.8 dB at Ø=0.7 and 103.7 dB at Ø=0.8. For the next two cases, two PIM rings of same ID were used. Results show that the total SPL with uniform ID rings increased at Ø=0.7 but decreased at Ø=0.8. Larger ID rings (Case 3) performed better than the smaller ID rings (Case 2), indicating that the flow area occupied by the PIM is an important design parameter. Next, PIM configurations in Figure 3 were examined, each with three PIM rings, a necessity to create the hyperbolic and elliptic shapes. Results show that the nozzle and hyperbolic configurations performed poorly. Elliptic and diffuser configurations produced similar total SPLs, but the diffuser was deemed more promising since it could also be formed with only two PIM rings to limit the flow restriction. Indeed, the diffuser configuration with 2 PIM rings (Case 8) yielded the best performance in this first series of experiments. In comparison with the baseline combustor, Case 8 decreased the total SPL by 2.7 dB at Ø=0.7 and by 7.0 dB at Ø=0.8.

Table 1. Total sound pressure levels for different test configurations.

CASE	Case Config.	Case Design	Total SPL (dB/dBA) Ø= 0.7	Ø= 0.8
1	No PIM	Baseline	**95.8/91.4**	**103.7/100.6**
2	Uniform area	d38p18-d38p18	100.4/94.8	101.0/97.3
3	Uniform area	d51p18-d51p18	96.4/91.3	98.9/95.2
4	Nozzle	d51p18-d51p18-d38p18	101.3/97.9	106.3/102.3
5	Hyperbolic	d51p18-d38p18-d51p18	101.7/98.5	103.4/100.1
6	Elliptic	d38p18-d51p18-d38p18	98.3/93.8	98.8/96.1
7	Diffuser	d38p18-d38p18-d51p18	97.8/87.7	99.1/95.5
8	Diffuser-2	d38p18-d51p18	**93.1/86.2**	**96.7/93.3**

Effect of Pore Density

Several diffuser configurations with different pore densities were examined, as shown in Table 2. A change in pore density from 18 ppcm to 8 ppcm (Case 2) deteriorated the performance since the interior combustion mode was readily established in the PIM with large pores (or small pore density). Next, the pore density of one of the rings was kept constant at 18 ppcm, while that of the other ring was varied to obtain a pore density gradient in the flow direction. For 18 ppcm PIM ring in the upstream, the SPL at Ø=0.7 was 93.1, 94.0, and 95.6 dB, respectively, for

downstream PIM ring of 18, 8, and 4 ppcm. In contrast, for 18 ppcm PIM in the downstream, the SPL at Ø=0.7 was 93.1, 96.1, and 98.5 dB, respectively, for upstream PIM ring of 18, 8, and 4 ppcm. These results show that a large pore density PIM (18 ppcm in this case) is more desirable, especially in the upstream region. A diffuser configuration with seamless, tapered wall was envisioned; however, PIM is a complex structure requiring specialized manufacturing process to control its thickness and shape. Diffuser-3 (Case 7) with three PIM rings of gradually increasing diameter approximates this idealized configuration. Table 2 shows reduction in the total SPL, especially in terms of dBA, for this diffuser configuration.

Table 2. Total sound pressure levels for different diffuser configurations.

CASE	Case Config.	Case Design	Total SPL (dB/dBA) Ø= 0.7	Ø = 0.8
1	Diffuser-2	d38p18-d51p18	**93.1/86.2**	**96.7/93.3**
2	Large pore, LP	d38p8-d51p8	100.9/96.0	101.1/98.9
3	Down-LP-8	d38p18-d51p8	94.0/85.9	97.0/93.1
4	Down-LP-4	d38p18-d51p4	95.6/90.4	97.7/94.8
5	LP-up-8	d38p8-d51p18	96.1/91.9	98.0/95.2
6	LP-up-4	d38p4-d51p18	98.5/94.9	99.5/96.5
7	Diffuser-3	d38p18-d44p18-d51p18	**92.1/82.2**	**97.3/92.4**

Conclusions

This study has shown that direct combustion noise can be reduced by passively manipulating the combustion process using PIM rings. The baseline combustor with no PIM rings produced total SPL of 95.8 dB (91.4 dBA) at Ø=0.7 and 103.7 dB (100.6 dBA) at Ø=0.8. The best performing PIM configuration reduced baseline noise levels by as much as 3.7 dB at Ø=0.7 and about 7.0 dB at Ø=0.8. Experiments revealed that PIM ring of diffuser shape is most effective for combustion noise reduction. In this study, the diffuser was formed with step changes in the flow area, but the ideal diffuser would be a seamless structure with tapered wall. Results show that a high pore density PIM (18 ppcm or higher) ring is necessary, especially in the upstream region, to effectively mitigate the combustion noise. High pore density PIM is also necessary to prevent combustion in interior mode and, hence, to safeguard against excessive heating of combustor surfaces, unexpectedly high sound pressure levels, and mechanical degradation of the PIM by repeated startup and shutdown.

References

[1] Bussman W & Jayakaran JD. (2001). Noise. The John Zink Combustion Handbook. C.E. Baukal (Ed), CRC Press, New York, Chapter 7.

[2] Lieuwen TC & Yang V (Eds). (2005). Combustion Instability in Gas Turbines: Operational Experience, Fundamental Mechanism and Modeling. Progress in Astronautics and Aeronautics, 210.

[3] Sequera D & Agrawal AK. (2009). Numerical Simulations of Swirl-Stabilized Combustion Coupled with Porous Inert Medium. Proceedings of the 6th U.S. National Combustion Meeting, Paper 11C3.

[4] Starhle WC. (1978). Combustion Noise. Progress in Energy and Combustion Science, 4:157-176.

[5] Wicksall DM & Agrawal AK. (2007). Acoustics Measurements in a Lean Premixed Combustor Operated on Hydrogen-Hydrocarbon Fuel Mixtures. International Journal of Hydrogen Energy, 32:1103-1112.

Larry "Justin" Williams is a senior from Phil Campbell, Alabama, majoring in mechanical engineering. For this paper, he conducted his research on porous media with Dr. Ajay Agrawal in the Department of Mechanical Engineering during the summer of 2009. Larry is a member of the Golden Key Honor Society, the Tau Beta Pi Engineering Honor Society, and the Pi Tau Sigma Mechanical Engineering Honorary. He is also the financial director for the Society of Automotive Engineers.

Synthesis and Modeling of Fluorescent Gold Nanoclusters

Lauren Wintzinger, Wei An, C. Heath Turner, Ph.D., * Yuping Bao, Ph.D.
*Faculty Sponsor

Department of Chemical and Biological Engineering, The University of Alabama, Tuscaloosa, AL 35487, USA

Fluorescent metallic nanoclusters (e.g., Au and Ag) with small numbers of metal atoms have great potential in bio-labeling and single molecule detection as fluorescent tags due to their extremely small sizes. Fluorescent Au and Ag nanoclusters are primarily produced inside large molecule templates with molecular weights of hundreds to thousands of Daltons. These templates not only increase the overall size of the nanocluster complexes, but also make it difficult to identify the cluster core sizes and nanocluster-ligand interfaces. Here, we report the successful production of fluorescent Au nanoclusters using two small (< 500 Daltons) biological molecules, L-ascorbic acid and 2-(N-Morpholino)ethanesulfonic acid (MES). We investigated how the synthetic parameters such as reaction temperature, concentration of the molecules, and pH effect the fluorescent emission of the Au nanoclusters. Further, we used electronic structure calculations to model and predict the geometric structure and HOMO-LUMO gaps of the nanocluster complexes.

Introduction

Fluorescence sensing and imaging techniques remain as the two primary methods for *in vitro* detection of molecules in solution and *in vivo* imaging of cells and cellular processes [7]. Unfortunately, the performance and sensitivity of these fluorescence techniques are greatly limited by the fluorescent tags attached to the biological or cellular components. Organic dyes are the most commonly used fluorescent labels, but their poor photostability leads to reduced sensitivity and decreased tracking lifetime of the targets. Their small Stokes shifts, difference between the absorption and emission wavelengths, also limit their use in multi-colored imaging [8]. In addition, most organic dye molecules cause aggregation in biological environments due to the hydrophobicity and salt effect [13]. Relative to organic dyes, semiconductor quantum dots have shown great promise in bio-labeling due to their valuable photophysical properties (i.e., size-tunable narrow emissions, large Stokes shifts, and minimal photobleaching) [5]. Unfortunately, the uses of quantum dots are limited by their harsh synthetic conditions, tedious surface passivation steps [6], and uncertain cytotoxicity *in vivo* [3].

The development of fluorescent metallic nanoclusters provides alternative labels for biological application [11,14]. One of the major advantages of these fluorescent tags is their extremely small size (< 1 nm), which does not disturb the biological functions of the labeled bio-entities. Currently, large molecules are mainly used as templates for the synthesis of fluorescent nanoclusters, such as polymers [1,15] or proteins [12]. These templates not only increase the overall size of the nanocluster complexes, but also make it difficult to identify the cluster core sizes and the details of the nanocluster-ligand interfaces. The tunable fluorescence emissions of the nanoclusters are mainly attributed to their size variation, according to the spherical Jellium model. This model was originally derived for gas phase alkali metal nanoclusters, stating that the transition energy is a function of the cluster size [9]. Unlike in gas phases, nanoclusters in solution are stabilized with ligands, the role of which is totally overlooked when using this model.

Here, we report the successful production of Au nanoclusters using small biological molecules such as L-ascorbic acid and 2-(N-Morpholino)ethanesulfonic acid (MES). L-Ascorbic acid is the scientific name of vitamin C, and MES is a biological buffer, commonly used for biological conjugation and assays. We found that the fluorescent emission of Au nanoclusters strongly depended on the concentration of the molecule in solution, and the optimized yield was related to the reaction temperature. Our simulated models of L-ascorbic acid stabilized Au nanoclusters suggested a three-atom nanocluster core.

Experimental

Chemicals

The biological buffer, *MES (2-(N-Morpholino)-ethanesulfonic acid*, pK_a=6.15) was purchased from Agros. The biological molecules, L-ascorbic acid and gold chloride, were purchased from Sigma Aldrich.

Synthesis of Au nanoclusters

Fluorescent Au nanoclusters were synthesized by first mixing a gold chloride aqueous solution with a biological molecule aqueous solution at room temperature. The concentration of the biomolecules was kept at 100 mM. The biomolecule to Au ratios were set to be 100:1, 10:1, or 1:1. The well-mixed reaction solution was then kept at a different temperature (25, 37, or 45 ^{o}C) in a shaking incubator. After incubation, a dark red solution was obtained, which contained a mixture of Au nanoparticles and fluorescent Au nanoclusters. The Au nanoparticles were removed by centrifugation (15,000 rpm), resulting in a clear Au nanocluster solution. The fluorescent emission of Au nanoclusters was studied as a function of molecule concentration and temperature.

Characterization of Au nanoclusters

The bulk fluorescence property of the Au nanocluster solution was analyzed on a Varian Cary Eclipse Fluorescence Spectrometer. Generally, both emission and excitation spectra were recorded to provide the optimum emission and absorption. All spectra were recorded using preset conditions (medium scan rate, medium detector PMT, and using a 3 mL volume cuvette).

Modeling of Au nanoclusters

Electronic structure calculations were performed on ascorbic acid stabilized Au nanoclusters, using the Gaussia03 software package [4]. The optimized geometry and the HOMO-LUMO gap of the nanocluster complexes were predicted using all-electron density-functional theory (DFT) with the generalized gradient approximation of the Becke three-parameter Lee-Yang-Parr (B3LYP) hybrid exchange-correlation functional [10,2].

Results and Discussion

Nanocluster emission analysis

Two typical fluorescence emission spectra of Au nanocluster solutions after centrifugation are shown in Figure 1. Gold nanoclusters stabilized with ascorbic acid exhibited maximum absorption/emission at 370 nm/450 nm, while MES stabilized clusters yielded maximum absorption/emission at 420 nm/495 nm. The ascorbic acid stabilized nanoclusters exhibited a bluish color under 365 nm UV light irradiation, and MES stabilized clusters showed a greenish color under mercury light irritation with a 405 ± 20 nm filter (Figure 1 inserts).

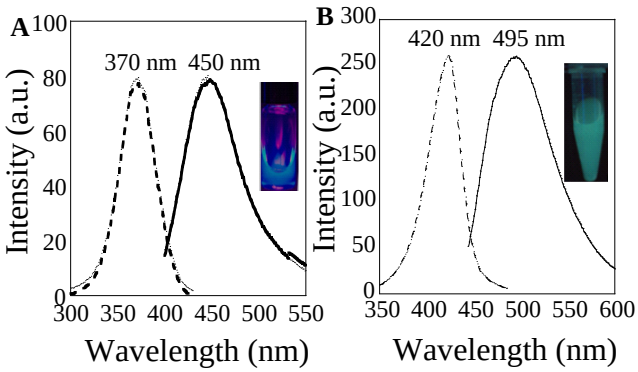

Figure 1. Fluorescence excitation (dashed line) and emission (solid line) spectra of Au nanoclusters, stabilized with biological molecules: (A) ascorbic acid and (B) MES. Insert photography was taken using a 365 nm UV lamp or mercury arc lamp with an emission filter of 405 ± 20 nm.

Simulation of nanoclusters

In the simulations, two optimized structures of the Au_3-ascobic acid complexes were obtained with either 2 or 6 ascorbic acid molecules attached to the nanoclusters (Figure 2). The shortest binding distance between the Au_3 nanocluster and the ascorbic acid in $Au_3(C_6H_8O_6)_2$ was $d_{Au\text{-}O}$ = 2.37 Å.

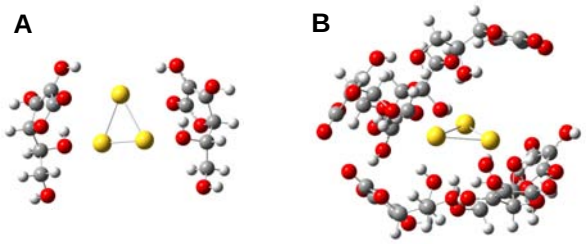

Figure 2. Geometry of ascorbic acid stabilized Au nanoclusters. (A) $Au_3(C_6H_8O_6)_2$ and (B) $Au_3(C_6H_8O_6)_6$.

In contrast, for $Au_3(C_6H_8O_6)_6$, a cage-like structure with six ascorbic acid molecules was predicted, mainly due to the formation of the intermolecular hydrogen bonds between the hydroxyl (–OH) groups ($d_{O-H\cdots O} = 2.73$ Å). This ascorbic acid cage structure was also proposed to contribute to the stabilization of the Au_3 nanoclusters (d_{Au-O} = 2.29Å), suggesting that the H-bonds play a key role in stabilizing the Au_3 nanoclusters.

The calculated HOMO-LUMO gaps for the complexes, $Au_3(C_6H_8O_6)_2$ and $Au_3(C_6H_8O_6)_6$, were 2.68 eV (462 nm) and 1.60 eV (775 nm), respectively. These numbers are significantly different from the HOMO-LUMO gap (1.29 eV) of bare Au_3, which indicates that the ligands indeed influenced the fluorescent emissions of the metallic nanoclusters. The HOMO-LUMO gap of $Au_3(C_6H_8O_6)_2$ was very close to our experimentally observed blue emission of 450 nm.

To experimentally confirm the formation of the hydrogen-bonded cage structure, we modified our experiments by increasing the ascorbic acid concentration and lowering the reaction temperature. Interestingly, we observed a red shift in the emission spectrum, as shown in Figure 3. Along with the blue fluorescent emission (465 nm), a broad shoulder around 560 nm (Figure 3 arrow) was observed, indicating the likelihood of the more cage-like structure at higher concentrations. The broader emission spectrum suggests the presence of multiple emissive species.

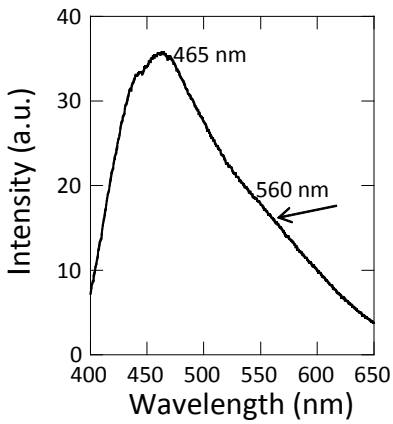

Figure 3. Fluorescent emission of ascorbic acid stabilized Au nanoclusters produced at high molecule concentration and low temperature.

Synthetic parameters

Using MES stabilized Au nanoclusters as a model system, we studied the effects of the synthetic conditions on the fluorescent emissions. Our experimental results show that the fluorescent emission intensity of the MES stabilized Au nanoclusters increased with the reaction temperature, suggesting a higher nanocluster yield (Figure 4A).

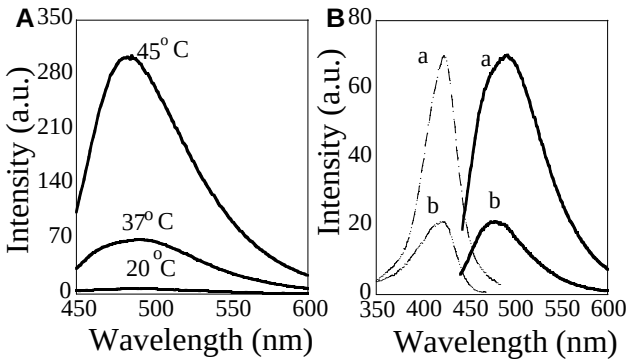

Figure 4. Fluorescent emission of MES stabilized Au nanoclusters at (A) different temperature and (B) different Au concentration at 37 °C.

Temperatures higher than 45°C were not pursued. For the targeted biological applications, the temperature is normally below 45°C. At the same reaction temperature, the yield of the nanoclusters increased with the Au concentration. Figure 4B shows the two emission spectra of Au nanoclusters synthesized at 37 °C for biological molecule to Au ratios of 10:1 (a) and 100:1 (b). Further increasing the Au concentration resulted in significant increases in the production of non-fluorescent Au nanoparticles, which significantly reduced the yield of fluorescent nanoclusters.

Conclusion

In summary, we report a new method for preparing fluorescent and water-soluble Au nanoclusters using small molecules as reducing agents and stabilizing ligands. The yield of the nanoclusters was strongly affected by the reaction conditions, such as temperature and concentration. Our simulation models for the different arrangements of molecules indicate that a mixture of species may have been present, resulting in different fluorescent emissions.

This study provides a starting point towards understanding the formation and stabilization of small size nanoclusters. Furthermore, our work may represent an inexpensive method for producing fluorescent species from bulk colloidal gold.

References

[1] Bao Y, Zhong C, Vu DM, Temirov JP, Dyer RB & Martinez JS. (2007). Nanoparticle-free synthesis of fluorescent gold nanoclusters at physiological temperature. J. Phys. Chem. C., 111:12194-12198.

[2] Becke AD. (1993). Density-functional thermochemistry. The role of exact exchange. J. Chem. Phys., 98:5648-5652.

[3] Chang E, Thekkek N, Yu WW, Colvin VL & Drezek R. (2006). Evaluation of quantum dot cytotoxicity based on intracellular uptake. Small, 2:1412-1417.

[4] Frisch MJ, e. a. (2004). Gaussian 03, Revision E.01, Gaussian, Inc., Wallingford CT.

[5] Gao XH, Chan WCW & Nie SM. (2002). Quantum-dot nanocrystals for ultrasensitive biological labeling and multicolor optical encoding. J. Biomed. Opt., 7:532-537.

[6] Gerion D, Pinauld F, Williams SC, Parak WJ, Zanchet D, Weiss S & Alivisatos A. (2001). Synthesis and properties of biocompatible water-soluble silica-coated CdSe/ZnS semiconductor quantum dots. J. Phys. Chem. B., 105:8861-8871.

[7] Ishikawa M, Maruyama Y, Ye JY & Futamata M. (2002). Single-molecule imaging and spectroscopy using fluorescence and surface-enhanced Raman scattering. J. Bio. Phys., 28:573-585.

[8] Jaiswal JK, Mattoussi H, Mauro JM & Simon SM. (2003). Long-term multiple color imaging of live cells using quantum dot bioconjugates. Nat. Biotechnol., 21:47-51.

[9] Kreibig U & Vollmer M. (1995). Optical Properties of Metal Clusters, Berlin: Springer-Verlag.

[10] Lee CT, Yang WT & Parr RG. (1998). Development of the Colle-Salvetti correclтion-energy formulor into a functional of the electron-density. Phys. Review B., 37:785-789.

[11] Lin CAJ, Yang TY, Lee CH, Huang SH, Sperling RA, Zanella M, Li JK, Shen JL, Wang HH, Yeh HI, Parak WJ & Chang WH. (2009). Synthesis, characterization, and bioconjugation of fluorescent gold nanoclusters toward biological labeling applications. ACS Nano, 3:395-401.

[12] Xie J, Zheng Y & Ying JY. (2009). Protein-Directed Synthesis of Highly Fluorescent Gold Nanoclusters. J. Am. Chem. Soc., 131:888-889.

[13] Yeung KW & Shang SM. (1999). The influence of metal ions on the aggregation and hydrophobicity of dyes in solutions. JSDC, 115:228-232.

[14] Zheng J, Nicovich PR & Dickson RM. (2007). Highly fluorescent noble-metal quantum dots. Ann. Rev Phys. Chem., 58:409-431.

[15] Zheng J, Zhang CW & Dickson RM. (2004). Highly fluorescent, water-soluble, size-tunable gold quantum dots. Phys. Rev. Lett., 93:077402-1-4.

Lauren Wintzinger is a sophomore from Huntsville, Alabama, majoring in chemical and biological engineering. She conducted her research for this paper in the laboratory of Dr. Yuping Bao in the Department of Chemical and Biological Engineering. Lauren is a Presidential Scholar and is on the Southeastern Conference Academic Honor Roll as a Division I Athlete. She is also a member of the Society of Women Engineers, Golden Key Honor Society, and the assistant coach of the UA Men's Club Volleyball Team.

Access to Safe Drinking Water in Cambodia: Available Sources and Point-of-Use Water Treatment

Marcus F. Aguilar
Faculty Sponsor: Joseph M. Brown, Ph.D.

Department of Civil, Construction, & Environmental Engineering, University of Alabama, Tuscaloosa, AL 35487, USA

Water is a resource that Cambodia has in abundance, but health problems persist in rural areas of the country due to unsafe drinking water. The Cambodian government in association with non-governmental organizations (NGO) and the private sector has promoted implementation of methods to filter and/or disinfect water at the point of use, but current programs have encountered obstacles. Engineers Without Borders at the University of Alabama visited the rural areas of Kampong Speu Province and Siem Reap Province, Cambodia to perform an observational study of potential drinking water sources and identify the problems the country faces in treating water for consumption using an in-home ceramic water purifier. Results suggest that typical drinking water sources are unsafe and that household water filtration is a useful but complex intervention strategy for addressing this problem.

Introduction

Cambodia is the poorest country in Southeast Asia and has the least developed infrastructure in the region, due partly to the recent history of genocide and conflict from the 1970s–1990s and the associated loss of investment and human capital [13]. The Khmer Rouge regime massacred from 2–4 million Cambodians, many of which were of the educated class, leaving the country with a lack of doctors, lawyers, engineers, teachers, and other trades that require formal training. Foreign investment and development has slowly returned to Cambodia, but 19% of Cambodians still subsist on less than 1 USD per day [12]. Infrastructure development and access remains low compared with neighboring countries.

Water is abundantly available in Cambodia, with the Mekong, Bassac, and Tonlé Sap Rivers as well as the largest freshwater lake in Southeast Asia in Tonlé Sap Lake, with an average surface area of 8,155 km^2 [2]. Available surface water resources are subject to large yearly fluctuations, as the country experiences the cycle of dry and rainy seasons. Groundwater is also widely available in most areas of the country, and has been accessed through both hand dug wells and the more advanced drilled wells with hand pumps. UNICEF, other donors and aid organizations have rapidly scaled up access to wells in rural areas. Groundwater is increasingly suspect as a source of drinking water in some areas due to arsenic contamination, however [3].

In spite of the high availability of drinking water sources in Cambodia, the lack of infrastructure development means the country faces serious challenges with respect to safe drinking water. An estimated 39% of the rural population of the country uses unimproved drinking water sources [14], and the danger of this is manifested in the Kingdom's high infant mortality rate of 82 per 1000 live births [18]. 56.2% of post-neonatal deaths in Cambodia are attributed (at least partly) to the onset of diarrhea caused by the consumption of unhealthy water [5]. Diarrheal disease is the number one cause of death in children under 5 years of age in Cambodia [9].

Engineers Without Borders at The University of Alabama (EWB-UA) visited Cambodia in May 2009 and completed an initial survey of drinking water in two rural areas. EWB-UA's objectives in these areas were (1) to assess safety of a variety of source waters of different types in rural Cambodia, and (2) to examine the use of one household-scale water treatment device, specifically the ceramic water purifier, now being used throughout Cambodia. To fulfill objective (1), EWB-UA focused on a specific area of Kampong Speu Province, in which to investigate the quality of typical drinking water sources in rural Cambodia. Although this area is relatively close to Phnom Penh, it does not enjoy the benefits of access to modern infrastructure. Cambodians in this province rely on surface water stored in detention ponds or protected or unprotected wells. Typically, individuals collect the

water themselves in buckets or other containers, or have water delivered to them by a tank vehicle. The two main measures the group used to assess the quality of selected water sources were thermotolerant coliform (TTC) bacteria and arsenic. TTC is a bacterial indicator of waterborne fecal contamination. Arsenic is an emerging problem found in groundwater sources in Southeast Asia, particularly in the Mekong delta region, and is naturally occurring [11]. The emergence of arsenic as a health problem in Cambodia has caused consumers to switch from ground water sources that are generally lower in microbial content to surface water sources that do not contain arsenic. However, surface sources are more likely to have high amounts of TTC. As a result, consumers are at a higher risk of diarrheal disease due to the consumption of low quality surface water [3]. The World Health Organization states that TTC should not be detectable in any 100 mL sample of water, and the level of arsenic must be below 10 ppb in order for the sample to be considered safe to drink [17]. Since 49.3% of Cambodia's rural population relies on unprotected ponds, rivers, streams, or wells for drinking water [2], treatment is usually required to make water safe. In rural areas, an emerging strategy for treating drinking water is point-of-use (POU) filtration, such as rapid sand or ceramic water purifiers (CWP) shown in Figure 1, which are household-scale water treatment technologies. Centralized treatment facilities have not been established in rural Cambodia [2].

Figure 1. The outside and inside of a ceramic water purifier.

Because large scale public treatment systems may be decades away for much of rural Cambodia, POU treatment options have been widely promoted and are identified as an effective option in both cost and removal capabilities. The CWP is a viable option, as it is produced by NGOs in-country with locally available clay and milled rice husks [8]. These two components are mixed and pressed into a clay pot, then fired and cured. The process of the firing burns out the rice husks, leaving a porous ceramic structure. Finally, the pot is coated with a solution of silver nitrate, a microbiocidal compound designed to increase the effectiveness of the filter by reducing bacteria and algae on contact. This ceramic pot is placed in a plastic receptacle which allows for safe storage of clean water. Then it is sold to consumers at a cost of around 10 USD [8]. The CWP has been found to consistently reduce *E. coli* and other bacteria in water by up to 99.99999%, with typical reductions of 99% in field use. It has a useful life of around five years, although implementers often suggest replacement after 1-2 years [15]. EWB-UA's objective (2) was fulfilled by investigating the use of the CWP as a POU method in Siem Reap Province.

The bio-sand filter is an intermittently operated slow sand filter that is similar in application to the CWP. The bio-sand filter is capable of 98% removal of TTC [10] and is also capable of removing arsenic at a rate of 87-96% [6]. This added benefit makes it ideal for use in Cambodia, though in the areas EWB-UA visited, the CWP was much more common. This POU method shares many of the same qualities as the CWP, and it is used by over 1.5 million people worldwide [10]

Disinfection through household chlorination is another option for POU treatment, although it is more effective as a secondary treatment following filtration. Chlorine is the most common disinfectant because it is cost effective and practical to apply through tablets or in liquid form. Free chlorine has a microbial baseline reduction of 99.9%, but as turbidity is lessened (through filtration or other methods), it is capable of microbial reduction up to 99.9999% [10].

Before filtration or disinfection was available, consumers would boil water prior to drinking to assure its safety, and the majority still does boil some or all of their drinking water [1]. This treatment is only effective if the consumers wait for the water to boil, and then cool before drinking. Boiling water is quantitatively prohibitive in that a family could not possibly boil more water at one time than their largest cooking container. Boiled water often also becomes contaminated during storage [1]. The

method is therefore effective from a purely removal standpoint but is not practical for the long-term.

Methods

EWB-UA tested water sources from lakes, wells, and rivers to assess drinking-water quality. Representative sources were identified by our partner NGO, Lien Aid, which has an active water development program across rural Cambodia. Water quality metrics were set by the group before surveying to evaluate the merits of each source.

These metrics provided a basic algorithm intended to identify water sources for present consumption and future development by Lien Aid, who is planning to build water treatment plants in the area. The team recorded a wealth of information for each site, including location (as indicated by GPS), road access, seasonality, access to the public, and any other notable information. These variables were measured by careful observation of each site and its surroundings by the team and by interviews with Cambodians who were familiar with the area. Three samples were taken from each source in order to measure TTC, arsenic, fluoride (sent away for analysis), and free and total chlorine for sources such as wells that may have been treated. The team measured TTC using a DelAgua test kit (DelAgua, Robens Centre, UK). This test consisted of a membrane filtration method. Once the samples were filtered, they were incubated at 44.5^{o}C +/- 0.5^{o}C on selective growth media. After approximately 18 hours, the TTC colonies can be visualized on the filtered graph paper (Figure 2).

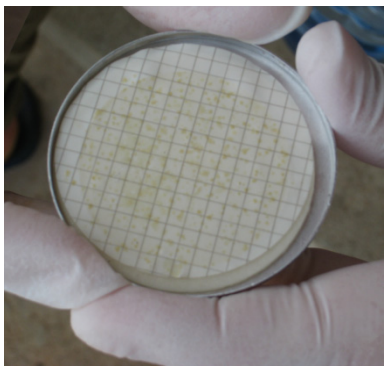

Figure 2. TTC count on filtered graph paper. TTC colonies represented by yellow blotches.

The test kit provided everything necessary for the process, with the added benefit of an internal battery that could sustain the incubation process even in areas of intermittent or non-existent power supply. The team used the arsenic Econo-Quick test kit to determine arsenic levels in source bodies. This simple colorimetric test required the mixture of the sample water with three reagents to form arsine gas, which was then detected and quantified by a strip of reactant paper. The results of these tests and the observational information are tabulated in Table 1.

EWB-UA then moved to the province of Siem Reap to perform a non-random survey and observational study of filter use by the residents of villages around the city. The purpose of this was to:

1. Assess the value of the ceramic water purifier to users.

2. Test the functionality of the filters in terms of actual removal and practical use.

3. Observe the practices of the subjects pertaining to the collection, filtration, and consumption of water for all uses.

The completion of these three objectives provides an understanding of the relationship that the rural Cambodian has with his or her CWP, and offers a glimpse of the wider issues related to the use of household water treatment in Cambodia. The survey consisted of an interview with the user and a collection of water samples at the input and output of each CWP. This allowed EWB-UA to connect each subject's behaviors pertaining to the filter with quantitative filter performance results. It also created an association between the necessity of filtration as revealed by the statistics from Kampong Speu, and the actual practice of filtration as observed in Siem Reap.

Results and Discussion

Each site had different qualities but, in general, the conclusion drawn from the survey is that rural Cambodians do not have access to clean drinking water, unless they venture to filter it themselves. Of the 22 drinking water sources (Table 1), only two of the sites met the WHO standard for safe drinking

water of 0 TTC colony forming units (cfu)/100 mL, and one sample was within the threshold of moderate risk (11-100 cfu/100 mL). All other samples (19 of 22) were classified as high risk sources (>100 cfu/100 mL) should they be consumed untreated. Since there are no large-scale drinking water treatment facilities in the province, it is left up to the consumers to practice POU water treatment (e.g., filtration or disinfection) to ensure that the water they drink will not make them sick.

The tested wells did not have results that were noticeably more favorable than any surface water source. Only one of the five wells with available TTC data met WHO standards, and one of the wells far exceeded the safe threshold for arsenic. Arsenic testing showed that low levels of this compound are present in the region, in the range of 0-25 ppb, but a low level indicator test is required to determine if these sites would actually meet the worldwide standard of 10 ppb. In general, all tested sites met the Cambodian national standard of 50 ppb, which is a performance-based standard [3].

Chanthual Lake and Krang Ambel Pond are potentially the best sources in Kampong Speu Province for the placement of a Lien Aid water treatment facility, based on year-round availability of water at those sites and good resident perception of the water quality. However, at present their TTC count is too high for consumption. EWB-UA sampled the water that a vendor was collecting at the Banteay Kmae pond, in which results indicated that it contained enough TTC to categorize it as a moderate-risk source. Vended water in the area is not subjected to regulation and is generally delivered untreated. Since consumers have no way of checking whether the water is safe to drink, this causes a potentially harmful situation. Centralized piped water that is treated to international standards would be a vast improvement over current conditions. Until that service is provided, residents of Kampong Speu Province and other rural areas will need to treat drinking water themselves using POU water treatment methods.

EWB-UA's work in Siem Reap (Supplementary Tables S1 – S3) identified existing problems with POU filtration of source waters. First, it was clear through the interview process that the subjects would be hesitant to reveal the full truth about their filter use.

Table 1. Results of site assessment in Kampong Speu Province, Cambodia.

Location	Water Source	Arsenic (ppb)	Thermotolerant Coliform Count (colonies/per 100 mL)
Psar Wat Ong	River	10	TNTC
Rolaing Sen Health Center	Well	25	391
Wat Ong Mi Trey	Spring fed	10	TNTC
Chanthual Lake	Lake, Fed by River	5	1767
Krang Ambel Village pond	Krang Ambel Channel	10	TNTC
Banteay Kmae	Rain Fed Pond	5	100
Krang Ambel Marsh	Rain Fed Pond	10	TNTC
Banteay Kmae Jr. High School	Tube Well	5	0
Phnom Pagoda Pond 1	Pond, Possibly Spring-Fed	10	TNTC
Okoki Village channel	Mountain Stream Fed	0	467
Phnom Pagoda Pond 2	Pond	10	4400
Kantuot Primary School Well	Tube Well	10	-
Wat Phnom Primary School Well 1	Tube Well	10	1000
Krang Mkak Village Well	Tube Well	5	-
Wat Phnom Primary School Well 2	Tube Well	10	300
Krang Mkak Village Pond	Pond	10	0
Prey Kvao Village Well	Tube Well	10	TNTC
Prey Tnot River	River	10	833
Pray Kvao Village Stream	Stream	0	3500
Thboung Ang Village Pond	Pond	10	7600

* TNTC – Too Numerous to Count

Instruction on the use, maintenance, and importance of the CWP was provided upon purchase of the filter,

and many of the subjects claimed to be following these guidelines closely. In several instances, however, EWB-UA found it highly unlikely that the subjects were truthful about the amount they used the filter. Interview number 1 (Supplementary Table S1), for example, started with the subject explaining that she used the filter daily and cleaned it regularly. After inspection of the filter and more thorough questioning, the subject admitted that the filter had not been used since the family left for the rice fields weeks earlier, and it had not been cleaned in at least one month. Furthermore, this subject did not believe that the well water was the cause of her diarrhea, stating that good taste was indicative of cleanliness. The subjects appeared to believe that it was better to imitate competence with the filter than provide actual information, a nuance that the interviewers realized almost immediately. This apparent disconnect between the subject's perception of the purpose of the interview, and the interviewer's desire for truthful answers, causes a problem that tends toward bias in surveys. When asked if the subjects were happy with the filter, all answered in the affirmative. However, when asked what they would make different about the filter, it was clear that they were not entirely satisfied with the performance of their CWP. Several explanations for these observations are possible. It is possible that the subjects expected further questioning if they did not answer in an appeasing manner, and they would have preferred to answer as few questions as possible. It is also possible that they associated the EWB-UA interview team with the NGO that taught them how to use the filters, in which they wanted to prove that they were responsible enough to merit their ownership of the filter. The subjects' hesitance to be forthcoming with the interviewers suggests that they have been taught how to use the filters without the benefit of knowing the importance of water sanitation. Strange explanations for how the filters function, as shown in interviews 11 and 13 (Supplementary Table S2), support this notion. The Khmer have survived for generations without water treatment. Providing them a filter and claiming that it will make them healthier is simply not enough to convince them of the importance of the CWP. User-focused, ongoing, participatory health and water education programs may help reinforce proper use of the filters.

Relevant to the consistency in which the subjects used their filters, EWB-UA discovered that for several months of the year, the Khmer do not use their filters simply because they are not at home. POU filtration works on the assumption that the user spends much of his/her time around the unit. Since Khmer families (or at least the men of working age) move to the rice fields, where they spend weeks on location raising a crop, the filter will most likely go unused by the absent parties in this time period. This fact is detrimental to the usefulness of the filter. Only one of the subjects that mentioned this problem suggested that it would be possible to take the filters to the fields, and it was evident that much disuse was due to this cause. An ephemeral solution to this problem would be to incorporate portability in the design of the CWP, possibly by adding handles and making it less susceptible to breakage. The answer to the cause of the problem, in reality, is that the subjects need to be more informed on the importance of the filters to their health. Local people must understand that drinking untreated water could cause sickness or death.

A complaint that occurred in 15 of the 37 interviews was that the CWP was too small, or the flow rate was too slow to maintain sufficient clean water for a family. The average number of children per family in Cambodia is 4.2, significantly higher than the world average of 2.6 [7]. A reasonable consumption estimate is 19.8 liters per day with 4.2 children, 2 parents, and an average consumption rate of 3.2 liters/person/day [4]. The optimal flow rate of the CWP is 1.8–2.5 liters/hour [8], so a family would have to run their filter anywhere from 7.9–11 hours each day, assuming it runs constantly, to provide sufficient drinking water for their family. This is not a realistic proposition for Cambodian families. The resolution of this problem ought to be investigated further by CWP suppliers.

Results from water sampling suggested the following points to our team. First, water quality testing can be challenging in technologically less developed countries without proper equipment. The team also noted that water testing methods that provide instant results would revolutionize water testing in such situations, providing consumers with information on water safety and the efficacy of treatment. Also, the CWPs are not always as effective

in situ as they are in a laboratory environment (lab studies have shown that CWPs are capable of 99.99999% reduction of coliform bacteria, see Introduction). Only three of the twenty samples that had valid results at the filter spigot met the WHO standard of 0 TTC colonies per 100 mL of water. Seven of the twenty samples had more colonies than could accurately be counted (upper detection limit of 300), and the remaining filters registered varying amounts of colonies. No correlation between consumer attitude and filter output results were apparent. However, the results collected suggest that actual filter performance in the home of the end-user was lower than expected. The total sample size of EWB-UA's survey was too small to make generalizations about overall CWP performance in Cambodia. However, it is sufficient to say that poor drinking water quality can persist even though a filter is used. Ultimately, our study was limited by a low sample size and interpretation problems for both the water quality data and the observational and interview data collected in households of users. We can conclude, however, that available sources of drinking water are unsafe and the use of a household filter may not be an effective intervention. Health and hygiene education and support to users will help in making this a more effective strategy for improving drinking water at the point of use.

Conclusion

The complexities of the issues that surround clean drinking water in Cambodia are related to environmental, social, and economic factors. The ceramic water purifier is one promising option for treating drinking water to potable standards, when properly used. Piped drinking water may be decades away in rural Cambodia. However, since Cambodia has sufficient water resources, the potential for water treatment is great. Although the CWP is capable of a high degree of microbiological performance, the results from EWB-UA's survey showed that ownership of a filter does not imply proper use or any use at all. The survey showed that lack of knowledge and apathy toward the filter marginalized its benefits. Communities would benefit from health and hygiene education in support of filter implementation projects.

Acknowledgements

The EWB-UA team would like to thank our hosts in Siem Reap who welcomed us into their homes and provided us the information to make this possible. We would also like to thank Ben Davis at ADRA Cambodia and his associates that translated and facilitated our work around Siem Reap. Also, the group sends thanks to the members of Lien Aid that worked with us in Kampong Speu. The members of EWB-UA that were part of the team in Cambodia were: Will Black, Billy Clark, Sonja Gregorowicz, Rebecca Midkiff, Andrew Magee, Ynhi Thai, Lissa Petry, Rob Quinney, Dr. Phillip Johnson, Dr. Joe Brown, and myself, Marcus Aguilar.

References

[1] Clasen TF, Thao DH, Boisson S & Shipin O. (2008). Microbiological Effectiveness and Cost of Boiling to Disinfect Drinking Water in Rural Vietnam. Environmental Science and Technology, 42:4255-4260.

[2] Darong C. (2007). Drinking Water Quality in Cambodia. UNESCAP. Accessed December 12, 2009 at: http://www.unescap.org/esd/water/publications/cd/escapiwmi/waterquality/drinking%20water%20quality%20in%20cambodia.pdf.

[3] Feldman P, Rosenboom JW, Mao S, Chea S, Peng N & Iddings S. (2007). Assessment of the Chemical Quality of Drinking Water in Cambodia. Journal of Water and Health, 5(1):101-116.

[4] Grandjean AC. (2005). Water Requirements, Impinging Factors, and Recommended Intakes. Nutrients in Drinking Water. World Health Organization, 1-27.

[5] National Institute of Public Health, National Institute of Statistics [Cambodia] & ORC Macro. (2006). Cambodia Demographic and Health Survey 2005. Phnom Penh, Cambodia and Calverton, Maryland, USA: National Institute of Public Health, National Institute of Statistics, and ORC Macro.

[6] Ngai T & Walewijk S. (2003). The Arsenic Biosand Filter (ABF) Project: Design of an Appropriate Household Drinking Water Filter for Rural Nepal –

Final Report. Massachusetts Institute of Technology and Stanford University, USA.

[7] Population Reference Bureau. (2003). Recent Fertility and Family Planning Trends in Cambodia. Accessed December 16, 2009 at: http://www.prb.org/Articles/2003/RecentFertilityandFamilyPlanningTrendsinCambodia.aspx.

[8] Resource Development International – Cambodia. (2009). Ceramic Water Filters at RDIC. Accessed December 16, 2009 at: http://www.rdic.org/waterceramicfiltration.htm.

[9] Rosenbloom JW, Ockelford J & Robinson A. (2007). Water Supply and Sanitation in Cambodia: Poor Access for Poor People. World Bank Water and Sanitation Program, 5-6.

[10] Sobsey MD, Stauber CE, Casanova LM, Brown JM & Elliot MD. (2008). Point of Use Household Drinking Water Filtration: A Practical, Effective Solution for Providing Sustained Access to Safe Drinking Water in the Developing World. Environmental Science and Technology, 42:4261-4267.

[11] Stanger GS, Truong TV, Le Thi My Ngoc KS, Luyen TV & Thanh TT. (2005). Arsenic in Groundwaters of the Lower Mekong. Environmental Geochemistry and Health, 27:341-357.

[12] The World Bank Group. (2009). Frequently Asked Questions About Poverty in Cambodia. The World Bank Group. Accessed December 19, 2009 at: http://web.worldbank.org/WBSITE/EXTERNAL/COUNTRIES/EASTASIAPACIFICEXT/CAMBODIAEXTN/0,contentMDK:20720197~pagePK:141137~piPK:141127~theSitePK:293856,00.html.

[13] The World Bank Group. (2009). Regional Fact Sheet from the World Development Indicators 2009 – East Asia and Pacific. Accessed December 19, 2009 at: http://siteresources.worldbank.org/DATASTATISTICS/Resources/eap_wdi.pdf.

[14] UNICEF. (2006). Cambodia Statistics. Accessed 14 December 19, 2009 at: http://www.unicef.org/infobycountry/cambodia_statistics.html.

[15] Van Halem D, van der Laan H, Heijam SGJ, van Dijk JC & Amy GL. (2009). Assessing the Sustainbility of the Silver-Impregnated Ceramic Pot Filter for Low-Cost Household Drinking Water Treatment. Physics and Chemistry of the Earth, 34:37-38.

[16] Vanderzwaag JC. (2008). Use and Performance of Biosand Filters in Posoltega, Nicaragua. University of British Columbia, Canada.

[17] World Health Organization. (2004). Water Drinking Guidelines. Accessed December 12, 2009 at: http://www.searo.who.int/EN/Section314_4295.htm#bacteriology

[18] World Health Organization. (2009). Cambodia. Accessed December 14, 2009 at: http://www.who.int/countries/khm/en/.

Marcus Aguilar is a December 2009 graduate of the University of Alabama from Houston, Texas. He graduated Magna Cum Laude with a Bachelor of Science in Civil Engineering, and he conducted his research for this paper during his undergraduate career. He was also a Presidential Scholar and a National Hispanic Merit Scholar.

Diblock Copolymers for Magnetically Triggered Drug Delivery Systems

Sarah M. Nikles[1], Jacqueline A. Nikles, Ph.D. [2], Jason S. Hudson[2], and *David E. Nikles, Ph.D. [1]
*Faculty Sponsor

1. Department of Chemistry, University of Alabama, Tuscaloosa, Alabama 35487-0336, USA
2. Department of Chemistry, University of Alabama at Birmingham, Birmingham, Alabama 35294-1240, USA

Our interest in building a magnetically triggered delivery vehicle for drug delivery has led to this study of the thermally triggered release of pyrene from the core of polymer micelles. Poly(ethylene glycol)-b-polycaprolactone diblock copolymers were dissolved in water at concentrations above the critical micelle concentration. DSC curves showed a melting endotherm peaking near 41°C, indicating the polycaprolactone core was crystalline. Pyrene added to the micelle core did not interfere with the crystallization. At temperatures below the melting point of the core, the pyrene was trapped in the core. When heated above the melting point of the core, the pyrene was released from the core to enter the continuous aqueous phase. This showed the potential for thermally triggered release from polymer micelles.

Introduction

Diblock and triblock copolymers containing hydrophilic blocks, e.g., poly(ethylene glycol) and hydrophobic blocks, either poly(propylene glycol) (PEO-PPO-PEO) [1], poly(L-histidine) (His-PEG) [2], polylactic acid (PEG-PLA) [3-6], poly(D,L-lactide-co-glycolide) (PEG-PLGA) [7,8], poly(β-benzyl-L-aspartate) (PEG-PBLA) [9], or polycaprolactone (PEG-PCL) [10-16] form micelles in aqueous solution at concentrations above the critical micelle concentration (CMC). The micelle cores can be loaded with a hydrophobic cancer drug, such as taxol [3, 5], or doxorubicin [10-12]. The drug can be released by a change in pH for pH responsive poly(L-histidine)-PEG polymer micelles [2]. For polymer micelles containing polyester blocks (i.e. PEG-PLA [3], PLA-PEG-PLA [5, 6], PEG-PLGA [8], or PEG-PCL [10-16]), hydrolytic degradation of the ester block erodes the polymer core, effecting drug release.

We seek to build a magnetically triggered drug delivery system for cancer chemotherapy based on PEG-PCL polymer micelles (Figure 1). The micelles, containing a payload of cancer drugs, will be injected into the blood stream and travel to the cancer site. The targeting moiety will allow the micelle to specifically bind to the surface of the cancer cell, thereby immobilizing the micelle at the cancer site. An external AC radio frequency magnetic field pulse will heat the magnetic nanoparticle, which in turn heats the crystalline core to its melting point. When the micelle core is melted, the cancer drug is free to move from the core, leaving the micelle and attacking the cancerous tissue. As long as the micelle core is melted, we expect the cancer drug to set up a dynamic equilibrium between being in the core and in the continuous aqueous phase outside the micelle. When the magnetic field pulse is discontinued, the micelle core will cool and crystallize, trapping any remaining cancer drug in the core. The drug would remain in the core until the next magnetic field pulse, when it would be free to leave the core again. This magnetically triggered drug delivery system would

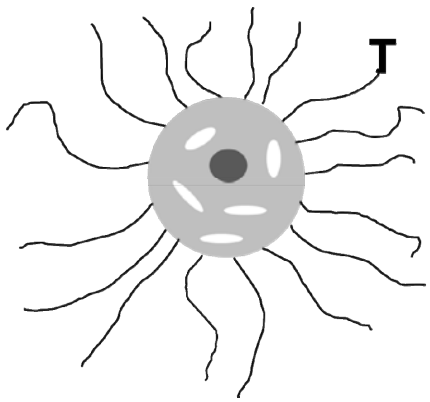

Figure 1. Schematic of a magnetically triggered drug delivery vehicle. The core contains a crystalline polymer (gray), a magnetic nanoparticle (black) and a trapped cancer drug (white). The micelle is dispersed in aqueous media by a hydrophilic polymer block (black curved lines). The micelle has a targeting moiety (black T) that specifically binds to cancer cells.

provide the oncologist an unprecedented spatial and temporal control of drug delivery, a powerful new tool for cancer therapy.

To create this drug delivery system, we must design polymer micelles with crystalline cores that can trap the cancer drug at physiological temperature (37°C). We chose polycaprolactone as the hydrophobic block because it is biocompatible, and its use *in vivo* is widely accepted [17]. Furthermore, polycaprolactone crystallizes with a melting point in the range of 40 to 50°C, just above physiological temperature. The cancer drug can be immobilized in between the crystallites in the micelle core and then be released when the core is melted. The enthalpy of melting would provide a thermal energy barrier against release at low temperature. Melting the polycaprolactone core would trigger the drug release. In this paper, we determined whether the polycaprolactone core in the micelles does indeed crystallize. We examined the effect of the incorporation of a small molecule on the ability of the polycaprolactone to crystallize. We also demonstrated release of the small molecule when the micelles were heated to temperatures above the melting point of the polycaprolactone core.

Experimental

Materials

ε-Caprolactone and dibutyltin dilaurate were purchased from Aldrich Chemical Company and used as received. Poly(ethylene glycol) monomethylether (M_n ~ 2,000) was also purchased from Aldrich Chemical Company. It was dried at 60°C in the vacuum oven overnight, allowed to cool to room temperature, and then stored in a dessicator over calcium chloride until used. The solvents were reagent grade and purchased from Fisher Scientific.

Synthesis of MeO-$(EG)_{36}$-$(CL)_{16}$-OH

A 250 mL three necked round bottom flask was dried in a glass drying oven overnight at 110°C. The flask was allowed to cool and was equipped with a reflux condenser, a thermometer, magnetic stirrer and a nitrogen atmosphere. Poly(ethylene glycol) monomethyl ether, M_n ~ 2,000 (20.00 g, 10.00 mmol), ε-caprolactone (22.80 g, 200.0 mmol) and dibutyltin dilaurate (0.10 mL) were added to the reactor and the reaction mixture was heated to 140 to 150°C using a silicon oil bath. The reaction mixture was allowed to stir at this temperature under nitrogen for 2.5 hours to give a viscous liquid. Afterwards, it was allowed to cool to room temperature whereupon the polymer solidified. The solid was taken up in a minimum amount of acetone, and enough hexane was added to the point of imminent precipitation. The solution was chilled in the refrigerator at 4°C overnight. The next day, the polymer had precipitated and was isolated by vacuum filtration. The polymer was rinsed with hexane and allowed to dry. Yield 28.53 g, 67%.

The other polymers reported here were synthesized using the same procedure, except the amount of ε-caprolactone was varied. For the case of MeO-$(EG)_{43}$-$(CL)_5$-OH, 5.70 g of ε-caprolactone (50.0 mmol) was used, while 11.40 g (100.0 mmol) was used for MeO-$(EG)_{40}$-$(CL)_9$-OH

Instrumentation

^{1}H NMR spectra of the polymers in $CDCl_3$ solution (Aldrich) were obtained on a Bruker Advance 360 Digital NMR. The degree of polymerization of the two blocks was determined for the integrated intensity of the resonances for selected peaks in the spectra. The critical micelle concentration was determined from the concentration dependence of the surface tension measured by the deNouy ring method using a Fisher manual model 20 surface tensiometer.

Results and Discussion

Diblock Copolymers

The diblock copolymers were made by the tin-catalyzed ring opening polymerization initiated from the alcohol terminus of poly(ethylene glycol) monomethylether. The molecular weight of the poly(ethylene glycol) was nominally 2,000, leading to the expectation that the degree of polymerization was 45. Integration of the peak for the terminal methyl group at 3.33 ppm (integral 3.00) and the methylene groups at 3.59 ppm (integral 138.7) gave a degree of polymerization of 35, indicating a molecular weight of 1570. The methylene groups in the polycaprolactone block had peaks at 1.37, 1.63, 1.52, 2.30 and 4.25 ppm, with the peaks at 1.63 and 1.52 ppm overlapping. The methylene group from the PCL block that links to the PEG block had a unique resonance at 4.17 ppm, thereby confirming the PCL

block was linked to the PEG block. As with the poly(ethylene glycol) monomethylether precursor, the PEG block had a resonance at 3.32 ppm for the terminal methyl group and a resonance at 3.59 ppm for the methylene groups. The integrated intensities of the peaks in the NMR were used to determine the degree of polymerization for each block (Table 1). The degree of polymerization for the PCL block was expected to be 5 for the first polymer, 10 for the second polymer, and 20 for the third polymer. Indeed, the degree of polymerization for the PCL block was 5 for the first polymer (MeO-$(EG)_{43}$-$(CL)_5$-OH), but was less than the expected degree of polymerization for the other two polymers. Notice that the degree of polymerization for the PEG block varied even though each used the same PEG starting material. We speculate that the purification procedure fractionated the polymers.

Table 1. PEG-PCL diblock copolymers.

Block Copolymer	M_n (g/mol)	CMC (mg/L)	CMC (M)
MeO-$(EG)_{43}$-$(CL)_5$-OH	~2,500	160	6.4×10^{-5}
MeO-$(EG)_{40}$-$(CL)_9$-OH	~2,800	46	1.6×10^{-5}
MeO-$(EG)_{36}$-$(CL)_{16}$-OH	~3,400	112	3.2×10^{-5}

The surface tension of aqueous solutions of the block copolymers was measured as a function of polymer concentration to give CMC values (Table 1), reported either as mg polymer per liter of solution or as moles per liter. The CMC of the diblocks was somewhat dependent on the length of the CL block.

MeO-$(EG)_{36}$-$(CL)_{16}$-OH was dissolved in water at a concentration of 2 mg/mL, well above the CMC. The solid, black DSC curve in Figure 2 shows a sharp melting endotherm that peaks at 41°C. This concentration is well above the CMC for this diblock. This provides strong evidence that PCL blocks in the core of the micelles crystallized.

Pyrene (0.010 mM) was added to an aqueous solution of 2 mg/mL MeO-$(EG)_{36}$-$(CL)_{16}$-OH (0.59 mM). This is a hydrophobic probe molecule that resides in the hydrophobic core of the micelle. The dashed DSC curve in Figure 2 shows the same sharp melting endotherm seen in the DSC curve for the micelles in the absence of pyrene. Indeed, the curves were almost superimposed. Clearly, the pyrene did not interfere with the ability of the polycaprolactone core to crystallize. This leads us to expect that a cancer drug would also not interfere with the ability of the polycaprolactone core to crystallize.

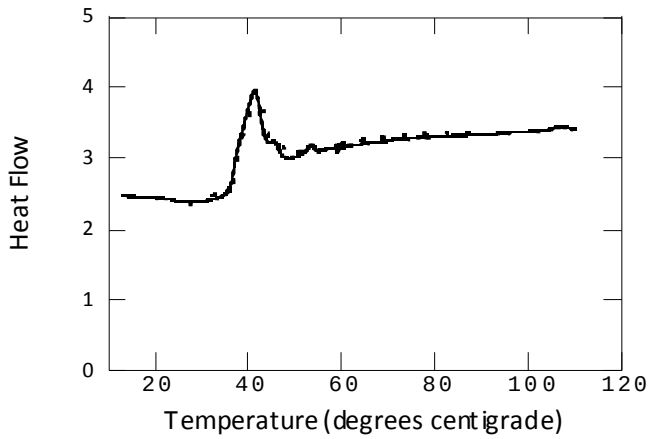

Figure 2. DSC curve for a 0.59 mM aqueous solution of MeO-$(EG)_{36}$-$(CL)_{16}$-OH, solid curve. The dotted curve is the DSC for the 0.59 mM MeO-$(EG)_{36}$-$(CL)_{16}$-OH solution containing 0.010 mM pyrene.

The capacity of the micelles to release a drug when heated was tested using pyrene (0.010 mM), a fluorescent probe, which was added to an aqueous solution of MeO-$(EG)_{36}$-$(CL)_{16}$-OH (0.59 mM). The fluorescence spectrum was measured during a 10°C/min ramp, with the fluorescence intensity at 374 nm shown as a function of temperature in Figure 3. In hydrophobic environments (e.g., inside the micelle), pyrene has a high fluorescence intensity, while in hydrophillic environments the fluorescence intensity decreases [18]. In the diblock copolymer, the pyrene was largely in the micelle core. However, as the temperature was increased above the melting point of the micelle core, the fluorescence intensity decreased, indicating that the pyrene had moved to a hydrophilic environment, the aqueous medium. Due to the temperature ramp used in this experiment, the release of pyrene happened quite fast as well. Similar results were obtained for the other polymers.

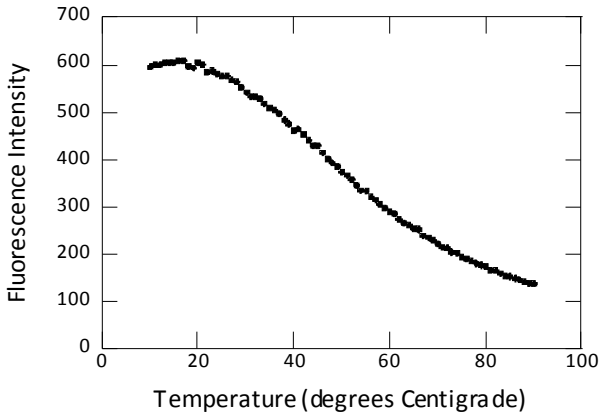

Figure 3. Fluorescence intensity at 374 nm as a function of temperature for pyrene in the presence of aqueous MeO-$(EG)_{36}$-$(CL)_{16}$-OH micelles.

Conclusion

Polymer micelles made from poly(ethylene glycol)-*b*-polycaprolactone diblock copolymers show promise for a magnetically triggered drug delivery vehicle. The polycaprolactone core was crystalline at temperatures below the melting point of the polycaprolactone. The DSC showed a sharp melting endotherm with a peak near 41°C. A small molecule was incorporated into the core, and its presence had little effect on the ability of the polycaprolactone to crystallize. The small molecule was released from the micelle core when the micelles were heated above the melting point of the core.

Our next task is to include magnetic nanoparticles into the core and determine whether they interfere with the ability of the core to crystallize. The last stage of our project will be to incorporate a cancer drug into the core and demonstrate magnetically triggered release.

Acknowledgements

The authors would like to thank Professor David E. Graves of the Department of Chemistry at UAB for allowing us to use his instruments.

References

[1] Almgren M, Bahadur P. Jansson M, Li P, Brown W & Bahadur A. (1992). Static and dynamic properties of a (PEO---PPO---PEO) block copolymer in aqueous solution. J. Coll. Interfac. Sci., 151(1):157-165.

[2] Lee ES, Shin HJ, Na K & Bae YH. (2003). Poly(L-histidine)–PEG block copolymer micelles and pH-induced destabilization. J. Control. Rel., 90:363-374.

[3] Zhang X, Jackson JK & Burt HM. (1996). Development of amphiphilic diblock copolymers as micellar carriers of taxol. Int. J. Pharm., 132:195-206.

[4] Chen W, Luo W, Wang S & Bei J. (2003**).** Synthesis and properties of poly(L-lactide)-Poly(Ethylene glycol) multiblock copolymers by coupling triblock copolymers. Polym. Adv. Technol., 14:245-253.

[5] Venkatraman SS, Jie P, Min F, Freddy BYC & Leong-Huat G. (2005). Micelle-like nanoparticles of PLA–PEG–PLA triblock copolymer as chemotherapeutic carrier. Int. J. Pharm., 298:219-232.

[6] Agrawal SK, Sanabria-DeLong N, Coburn JM, Tew GN & Bhatia SR. (2006). Novel drug release profiles from micellar solutions of PLA–PEO–PLA triblock copolymers. J. Control. Rel., 112:64-71.

[7] Yang J, Lee C-H, Park J, Seo S, Lim E-K, Song YS, Suh J-S, Yoon H-G, Huh Y-M & Haam S. (2007). Antibody conjugated magnetic PLGA nanoparticles for diagnosis and treatment of breast cancer. J. Mater. Chem., 17:2695-2699.

[8] Bae Y, Diezi TA, Zhao A & Kwon GS. (2007). Mixed polymeric micelles for combination cancer chemotherapy through the concurrent delivery of multiple chemotherapeutic agents. J. Control. Rel., 122:324-330.

[9] Kataoka K, Matsumoto T, Yokoyama M, Okano T, Sakurai Y, Fukushima S, Okamoto K & Kwon GS. (2000). Doxorubicin-loaded poly(ethylene glycol)–poly(β-benzyl-L-aspartate) copolymer micelles: their pharmaceutical characteristics and biological significance. J. Control. Rel., 64:143-153.

[10] Allen C, Han J, Yu Y, Maysinger D & Eisenberg A (2000). Polycaprolactone–*b*-poly(ethylene oxide) copolymer micelles as a delivery vehicle for dihydrotestosterone. J. Control. Rel., 63:275-286.

[11] Soo PL, Luo L, Maysinger D & Eisenberg A. (2002). Incorporation and Release of Hydrophobic Probes in Biocompatible Polycaprolactone-*block*-poly(ethylene oxide) Micelles: Implications for Drug Delivery. Langmuir, 18: 9996-10004.

[12] Shuai X, Ai H, Nasongkla N, Kim S & Gao J. (2004). Micellar carriers based on block copolymers of poly(ε-caprolactone) and poly(ethylene glycol) for doxorubicin delivery. J. Control. Rel., 98:415-426.

[13] Soo PL, Lovric J, Davidson P, Maysinger D & Eisenberg A. (2005). Polycaprolactone-*block*-poly(ethylene oxide) Micelles: A Nanodelivery System for 17β-Estradiol. Molecular. Pharm., 2(6): 519-527.

[14] Xie W, Zhu W & Shen Z. (2007). Synthesis, isothermal crystallization and micellization of mPEG–PCL diblock copolymers catalyzed by yttrium complex. Polymer, 48:6791-6798.

[15] Chausson M, Fluchére A-S, Landreau E, Aguni Y, Chevalier Y, Hamaide T, Abdul-Malak N & Bonnet I. (2008). Block copolymers of the type poly(caprolactone)-*b*-poly(ethylene oxide) for the preparation and stabilization of nanoemulsions. Int. J. Pharm., 362:153-162.

[16] Cho HK, Lone S, Kim DD, Choi JH, Choi SW, Cho JH, Kim JH & Cheong IW. (2009). Synthesis and characterization of fluorescein isothiocyanate (FITC)-labeled PEO–PCL–PEO triblock copolymers for topical delivery. Polymer, 50:2357-2364.

[17] Nair LS & Laurencin CT. (2007). Biodegradable polymers as biomaterials. Prog. Polym. Sci., 32:762-798.

[18] Kwon G, Naito M, Yokoyama M, Okano T, Sakurai Y & Kataoka K. (1993). Micelles based on AB block copolymers of poly(ethylene oxide) and poly(.beta.-benzyl L-aspartate). Langmuir, 9:945-949.

Sarah Nikles is a senior from Tuscaloosa, Alabama, majoring in biochemistry with a minor in mathematics. She works in the laboratory of Dr. David Nikles in the Department of Chemistry, where she conducted all of the research for this paper. Sarah has received a President's Cabinet Scholarship, was named a Semi-Finalist for the Siemens Westinghouse Science and Technology Competition for 2004-2005, and is a member of the Gamma Sigma Epsilon Chemistry Honor Society.

Attachment of AEAPT to Single Crystal Magnetite Nanoparticles for Future Tagging of Adenovirus

A. Kirstin Sockwell, Jeremy S. Pritchett, *David E. Nikles, Ph.D.
*Faculty Sponsor

Department of Chemistry, The Unversity of Alabama. Tuscaloosa, Alabama 35487-0336, USA

A mode of labeling adenovirus or herpes simplex virus with magnetic nanoparticles was created for MRI enhancement and magnetic hyperthermia therapy. The particles will enhance the MRI while the virus will target the cancerous tissue. Magnetic oxide nanoparticles were prepared with a covalently bound N-(2-aminoethyl)-3-aminopropyltriethoxysilane (AEAPT). Single crystal magnetite, cobalt ferrite, and nickel ferrite were made by literature procedures. The particles had a narrow distribution of particle sizes in the range of 5 to 10 nm. The AEAPT was bounded to the particles using sol-gel chemistry. Cu^{2+} was bounded to the AEAPT, and this provided a means for binding the particles to histidine tagged adenonvirus or tegument proteins.

Introduction

Cancer remains one of the leading causes of death. The National Institutes of Health has indicated that nanomedicine is an effective approach for cancer research [1]. Multifunctional nanoplatforms can target, detect, and report the efficacy of treatment. In this report, we describe our research to build new tools for nanomedicine.

Magnetic resonance imaging (MRI) is an important diagnostic tool for cancer. MRI maps the spatial distribution of proton relaxation times, either T_1 or T_2. Protons in different tissues have different relaxation times, providing a basis for imaging the tissues. Magnetic nanoparticles, by virtue of the local magnetic fields around the particles, bring a dramatic change in relaxation times (particularly T_2) for nearby protons. These nanoparticles can enhance the MRI contrast, allowing more sensitive detection of cancerous tissue [2].

When magnetic nanoparticles are subjected to a radio frequency AC magnetic field, the particles are heated by magnetic induction. The magnetic fields can penetrate deep into tissue without adverse effects on healthy tissue. If the magnetic particles were bounded to cancerous tissue, they could potentially kill it by hyperthermia therapy. Even if the heating were not enough to kill the cells, hyperthermia enhances the cytotoxicity of chemotherapeutic agents, creating a more efficient cancer treatment [3].

It is important to devise methods for nanoparticles to identify and attach to tumor tissue, which is a central challenge in cancer therapy. Collaborators at The University of Alabama in Birmingham (UAB) School of Medicine have engineered an adenovirus to target specific cancer cells [4], while colleagues in the UAB Department of Biological Sciences have created a herpes simplex virus to target brain cancer cells. Both groups are working to label the viruses with polyhistidine tags (his-tags). These are sequences of histidine residues that are placed on the hexon surface of the adenovirus capsid. Alternatively, the hist-tags would be placed in the tegument proteins that assemble the protein coating around the capsid for the herpes simplex virus. Here, we present methods for binding magnetic nanoparticles to these viral vectors. In both cases, a functional group must be attached to the particle for it to bind to the his-tags. Magnetite was chosen since it is approved for use *in vivo* [5].

Experimental

All chemicals were reagent grade or higher. Iron(III)acetylacetonate, 1,2-hexadecanediol, benzyl ether, oleic acid, oleylamine, [3-(2-aminoethylamino)-propyl]trimethoxysilane (AEAPT), copper(II) acetate, and nickel chloride were purchased from the Aldrich Chemical Company and used as received. Ethanol and dimethyl sulfoxide (DMSO) were purchased from Fisher Scientific.

Synthesis of 4 nm Fe_3O_4 Nanoparticles

Iron(III) acetylacetonate ($Fe(acac)_3$, 0.706g), 1,2-hexadecanediol (2.58g), benzyl ether (20 mL), oleic

acid (1.9 mL), and oleylamine (2.0 mL) were heated and magnetically stirred under constant nitrogen in a three-neck 50 mL round bottom flask. The mixture was heated to 200° C for 30 minutes and then heated to reflux (~300°) for 2 hours, creating a black brown solution. The solution was allowed to cool to room temperature by removing the heat source and nitrogen. Ethanol (40 mL) was added to the mixture, and it was centrifuged (15 min) to isolate a black, solid precipitate. The precipitate was dispersed in a mixture of hexane (20 mL), oleic acid (0.05 mL), and oleylamine (0.05 mL). The solution was sonicated to ensure complete dispersion then centrifuged (15 min). Ethanol (20 mL) was added, and the mixture was centrifuged again (15 min) to isolate the black precipitate. This hexane/ethanol washing process was repeated several times (4-5). The particles were stored in hexane.

Addition of AEAPT to Nanoparticles

Ethanol was added to the previously prepared particles in order to draw off the hexane. The solution was centrifuged until a solid was precipitated, and the clear liquid was removed. A 10% solution of AEAPT in DMSO was prepared by adding 9 mL DMSO to ~1 mL AEAPT in a 25 mL Erlenmeyer flask. The AEAPT solution was added to the sample, and the mixture was heated under constant stirring to ~80°C for 2 hours. The solution was allowed to cool to room temperature. It was centrifuged for 15 minutes or until a precipitate appeared. The amber brown liquid was decanted, leaving only the particles. Absolute ethanol was added to the particles. The sample was sonicated to remove any unreacted AEAPT. The ethanol/particle solution was centrifuged for 5 minutes, and a clear liquid was decanted. The particles were then dispersed in deionized (DI) water. A solution of 0.1 M copper acetate was made by dissolving 0.185 g copper acetate powder in 10 mL of DI water. The copper acetate solution was added to the particles, sonicated until complete dispersion, and centrifuged for 5 minutes. The particles were removed and allowed to dry.

Particle Characterization

Samples for x-ray diffraction (XRD) were prepared using the following procedure. The hexane-dispersed particles were washed by adding ethanol to the hexane until it became cloudy. The sample was centrifuged (15 mins), and the clear liquid was decanted. A minimum amount of hexane was added followed by sonication. This wash removed any oleic acid and oleylamine from the particles which may have remained from the synthesis. A smaller amount of hexane produced a denser liquid/particle ration. A silicon wafer was washed with acetone and methanol then air dried. About 5 drops of the particles were applied to the wafer and allowed to dry. This step was repeated until a dark coating appeared on the wafer. The sample was ran at 40 kV and 35 mA. The XRD covered from 20° to 80° using Cu K_α radiation, $\lambda = 154$ pm. After the XRD was completed, the silicon wafer was washed with hexane to remove the particles.

Infrared spectroscopy (IR) was conducted on the magnetite particles and the particles attached to AEAPT. The samples were analyzed on a ZnSe crystal. The sample of magnetite particles was washed using the same methods described for XRD and was either dispersed in hexane or methanol. The particles were then dropped onto the crystal and allowed to dry until a dark coating was produced. The sample with the particles attached to AEAPT was dispersed in methanol. The liquid was then dropped onto the crystal and allowed to dry until the surface appeared dark. After IR spectroscopy, the crystal was washed with methanol into a beaker. The collected content was then centrifuged in order to remove the particles. The samples were ran on a JASCO FT/IR-4100 Fourier Transform Infrared Spectrometer.

Samples for transmission electron microscopy (TEM) were prepared by dropping a dispersion of the particles onto carbon-coated TEM grids, and the hexane was allowed to evaporate.

Results and Discussion

Nanoparticle Synthesis

Magnetite nanoparticles were prepared by the thermal decomposition of iron(III)acetylacetonate in benzyl ether with oleylamine and oleic acid capping ligands. This followed a literature procedure by Sun *et al.* [6]. The x-ray diffraction curve in Figure 1 shows the expected diffraction peaks for magnetite (Table 1), giving a cubic lattice with a unit cell dimension a = 838.8 pm. Scherrer analysis of the line width of the most intense peak (311) gave an average crystallite

Table 1. X-ray diffraction peaks observed for the magnetite nanoparticles.

2θ	Miller Index
30.12	220
35.45	311
43.09	400
53.42	422
56.98	333
62.55	440

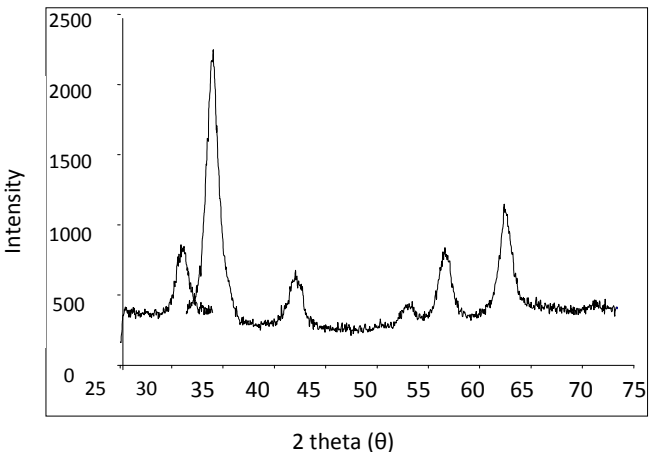

Figure 1. X-ray diffraction curve of the magnetite nanoparticles. Plot of intensity as a function of 2θ.

size of 7 nm. The procedure gave single crystal particles (Figure 2) with diameters in the range of 4 to 8 nm. The distribution of particle sizes was a bit broader than expected. However, the procedure provided enough particles for our purposes.

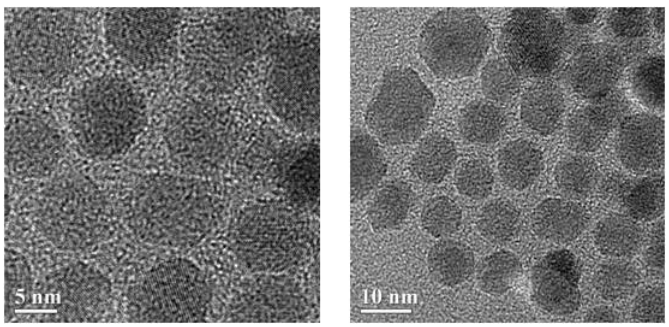

Figure 2. TEM images of magnetite particles between 4 nm and 8 nm.

A series of experiments on the reaction scale were done, where the batch size was doubled and then quadrupled. In each case, the yield doubled or quadrupled, as expected. The quality of the particles obtained from the larger batches was not affected.

Addition of AEAPT to Nanoparticles

AEAPT was bounded to the surface of the magnetite nanoparticles using a modified literature procedure described by Hung *et al*. [7]. The infrared spectrum for the particles after reaction with AEAPT is shown in Figure 3. Some unbounded AEAPT may have appeared in the 1350-1450 cm^{-1} range. The broad peaks in the spectrum around 3250 cm^{-1} and 3400 cm^{-1} are indicative of the NH_2 stretching mode of the AEAPT ligand. The sharp peaks around 2900cm^{-1} and 2850 cm^{-1} are characteristic of the CH_2 stretching mode.

The broad peaks around 1550 cm^{-1} and 1650 cm^{-1} suggest the NH bending mode. The sharp peaks around 1380 cm^{-1} and 1450 cm^{-1} are indicative of the CH_2 mode, and the broad peaks around 950 cm^{-1} and 1050 cm^{-1} are indicative of the Si-O-R stretching mode. The spectrum in Figure 3 suggests the successful attachment of the AEAPT ligand to the magnetite particles.

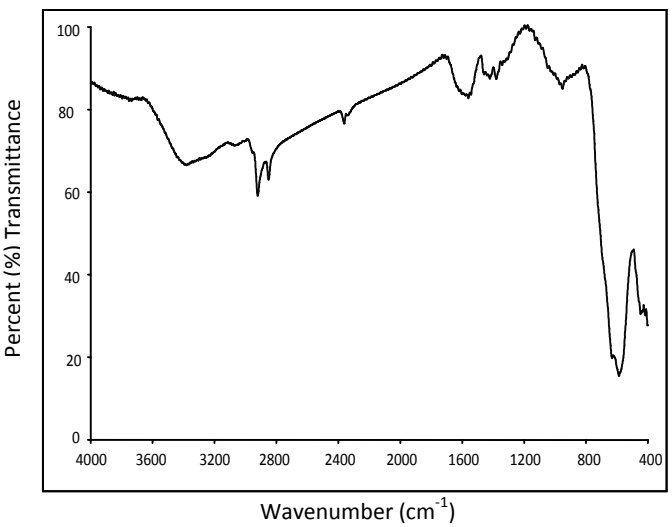

Figure 3. Infrared spectrum of the magnetite particles with AEAPT. Plot of percent transmittance as a function of wavenumber (cm^{-1}).

Conclusion

In summary, we prepared magnetite nanoparticles with the linker AEAPT bounded to the particle surface. The process is convenient and lends itself to scale-up, thereby allowing us to provide adequate quantities for magnetically labeling viruses. The silane coupling agent chemistry will work with other magnetic oxide nanoparticles, such as maghemite, cobalt ferrite, manganese ferrite, or nickel ferrite. Although we used Cu^{2+}, this chemistry allows the possibility to vary the choice of transition metal ion with other ions that could also bind the imidazole groups from the polyhistidine residues, including Ni^{2+}, Co^{2+} or Fe^{2+}. This provides a wide range of options for tailoring the linker to bind polyhistidine tags onto viruses.

References

[1] National Institutes of Health. NIH Common Fund: Nanomedicine.(2009). Accessed at: http://nihroadmap.nih.gov/nanomedicine/.

[2] Friedman BR. (1989). Principles of MRI. McGraw-Hill, New York, NY.

[3] Mohanned F, Stuart OA, Glehen O, Urano M & Sugarbaker PH. (2004). Docetaxol and hyperthermia: factors that modify thermal enhancement. J. Surg. Oncol., 88:14-20.

[4] Nettelbeck DM & Curiel DT. (2003). Tumor-busting viruses, Sci. Amer., 289(4):68-75.

[5] Murthy SK. (2007). Nanoparticles in modern medicine: State of the art and future challenges. Int. J. Nanomedicine, 2(2):129-141.

[6] Sun S, Zeng, H, Robinson DB, Raoux S, Rice PM, Wang SX & Li G. (2004). Monodisperse MFe_2O_4 (M = Fe, Co, Mn) nanoparticles). J. Am. Chem. Soc., 126: 273-279.

[7] Hung C-W, Holoman TRP, Kofinas P & Bentley WE. (2008). Towards oriented assembly of proteins onto magnetic nanoparticles." Biochem. Eng. J., 38:164–170.

Kirstin Sockwell is a sophomore from Pinson, Alabama with a major in chemistry. She currently works in the laboratory of Dr. David Nikles in the Department of Chemistry through the Emerging Scholars Program, in which she serves as a mentor for the freshmen class of Scholars. She has presented her research at The University of Memphis, and she is a Presidential Scholar.

Turning Back the Cellular Clock – A Review of Induced Pluripotent Stem Cells

Paige M. Dexter
Faculty Sponsor: Guy A. Caldwell, Ph.D.

Department of Biological Sciences, University of Alabama, Tuscaloosa, AL 35487, USA

Within the last decade, few areas of scientific research have been surrounded by as much excitement and controversy as stem cell research. Hailed as a potentially priceless tool in medical investigation, stem cells are able to transform into any type of cell in the body. Due to this unique capability, stem cells are seen as an attractive resource for use in medical research, especially in modeling diseases and screening drugs using cultured human tissues. During the past four years, researchers have developed techniques for artificially obtaining stem cells from donated adult tissue. Initially, these "induced pluripotent" stem (iPS) cells were reprogrammed using viral vectors to deliver certain factors that return the cells to a pre-differentiated state, but the presence of viral vectors increases the risk of dangerous genetic dysfunction in the cells. Methods of generating safe iPS cells without using viral vectors are being explored. Currently, the creation of patient-derived iPS cells suitable for use in clinical research and perhaps even tissue replacement therapy seems within reach. This paper reviews the milestones of iPS cell research to date, details current methods of deriving iPS cells, and introduces some recent advances that have been made in the field.

Introduction

The phrase "stem cell" actually describes all cells that have the potential to develop into different cell types through a process called "differentiation." There are three different kinds of stem cells, each with unique characteristics [8].

Embryonic stem (ES) cells are referred to as "pluripotent," or able to differentiate into any cell type in the body. Under certain conditions, ES cells are capable of prolonged self-renewal without differentiation, allowing long-term culturing of stem cells for research purposes [3]. However, due to the method by which ES cells are obtained, their use in medical research has troubling moral implications for many people. Most ES cells are derived from 4- to 5-day-old human embryos produced for *in vitro* fertilization then donated to research. The process destroys the embryos, a consequence that many view as morally objectionable. ES cell-related research has been hindered by these ethical concerns [8].

Adult stem (AS) cells are found in many different tissues, including bone marrow, blood vessels, skeletal muscle, adipose tissue, and the brain. Perhaps better termed as "somatic stem cells" since they are present in adolescents as well as adults, AS cells are used by the body for constant renewal of specialized cells. The use of AS cells in research to avoid the ethical concerns surrounding ES cells has been explored. However, their capacities for self-renewal and differentiation are inferior to those of ES cells, and they are considered a less desirable subject for medical research [8].

Induced pluripotent stem (iPS) cells are a relatively recent development that may circumvent the shortcomings of both ES and AS cells. In 2006, researchers at the Institute for Frontier Medical Sciences at Kyoto University demonstrated a method to convert mouse fibroblasts into iPS cells, eliminating the need for the destruction of a donor embryo. This technology enables researchers to engineer pluripotent stem cells from differentiated tissue, essentially turning back the cell's biological clock to a pre-differentiated state [9, 10].

The ability of stem cells to transform into any cell type represents a unique resource for medical researchers. Many possible roles for stem cells have been anticipated, including disease modeling and drug discovery using cultures of affected tissues in the lab. A more distant, but still highly anticipated, use for stem cells is in cell replacement therapy through transplantation of genetically modified iPS cell-derived tissues. This proposal is made even more attractive by the fact that a patient's immune system will likely not reject iPS cells derived from their own tissue, thus avoiding a serious concern in other transplantation procedures [3].

The Discovery of Induced Pluripotent Stem Cells

The term "iPS cell" was coined by Yamanaka and Takahashi in a landmark 2006 paper, in which they demonstrated a method for transforming mouse fibroblasts into pluripotent stem cells. Their procedure involved introducing certain transcription factors known to maintain pluripotency in ES cells to the fibroblasts using retroviral transduction. They found that the introduction of just four factors, Oct3/4, Sox2, c-Myc, and Klf4, was enough to return the cell to a pluripotent state [9].

Shortly after this discovery, the team utilized the same technique in human fibroblasts and produced human iPS cells. This result indicates that the network of transcription factors controlling pluripotency is essentially conserved between mice and humans. The researchers demonstrated their iPS cells to be similar to ES cells in many areas, including gene expression, morphology, proliferation, and ability to differentiate [10].

These cells have undergone other stringent tests for pluripotency and similarity to ES cells. In a study published in July 2007, it was noted that the artificially-engineered stem cells' chromatin state and DNA methylation were similar to that of ES cells. Additionally, iPS cells have been implanted into mice to stimulate the formation of teratomas, or growths containing cells from all 3 germ layers [11].

The most compelling evidence for the transformative potential of iPS cells has emerged very recently. In 2009, Zhao *et al*. generated litters of live offspring from mouse iPS cells through a process called "tetraploid complementation." In this procedure, virally-induced iPS cells from mouse fibroblasts were injected into a blastocyst. The resultant embryo was implanted into a mouse that later gave birth to live pups that were clones of the original skin cell donor. This result shows that, since the iPS cells are capable of producing healthy, living offspring after implantation, they are indeed able to regenerate every tissue type in the body. However, despite these promising findings, much of the exact relationship between ES and iPS cells still remains to be seen [14].

Non-viral Methods of Inducing Pluripotency

IPS cells engineered by integration of viral vectors into the cells' genes are unsuitable for clinical applications. Viral vectors must be active during the initial reprogramming stage of generating iPS cells. However, after pluripotency has been achieved, their expression is no longer needed [9]. These vectors, which are inserted into the genome of the cells, are capable of turning back on random and altering normal gene expression in the cells. This could distort the results of genetic and drug screens, rendering experimental results useless. In extreme cases, the location of vector integration may disrupt normal gene functions and lead to cancer [10]. Researchers are searching for ways to dedifferentiate adult cells without using viral vectors that must permanently integrate into the host cell's genome.

One proposed method uses transient transfection of expression plasmids coding for the transcription factors required to induce pluripotency. This 'nonintegration method' utilized an adenovirus-mediated gene delivery system, and the adenoviral vector showed no signs of integrating into the host genome [5].

Another technique uses doxycycline-inducible lentiviral vectors to control the expression of reprogramming factors and subsequently excises the virus using Cre-recombinase. This procedure has yielded iPS cells free of reprogramming factors that have been used to produce dopaminergic neurons from iPS cells derived from the fibroblasts of five Parkinson's disease patients. These cells displayed a gene expression profile more closely related to ES cells than iPS cells containing viral integrations [7].

Yet another technique utilizes transposons, mobile genetic elements that insert themselves into the genome to deliver the reprogramming factors. These genomic additions are removed by the enzyme transposase once pluripotency has been attained. The *piggyBac* transposon/transposase system has been used to create both mouse and human iPS cells that have passed rigorous tests for similarity to ES cells [13].

Other researchers have eliminated genome manipulation and DNA transfection altogether by delivering the reprogramming proteins themselves into human somatic cells. This method takes advantage of a peptide able to traverse the cell membrane to deliver the proteins to the cells. Though this procedure has successfully engineered iPS cells without genetic manipulation, the process was

extremely inefficient compared to viral transduction [2].

These methods and more have proven that viral integration is unnecessary to reprogram cells, but they remain slow and inefficient means of iPS cell production [14]. Furthermore, methods that involve the integration and later removal of reprogramming genes can still alter the cells' function at a genetic level. More research is required before non-viral methods of dedifferentiation can be used to generate iPS cells with the same efficacy as viral transduction [7].

Current Research and the Potential of iPS Cells

Although most research involving iPS cells to date has involved creating safer and more efficient protocols for producing them [3], investigation into their potential medical applications has yielded exciting results. Researchers at the University of Washington in Seattle have engineered photoreceptors from human iPS cells that can be implanted into mouse models for retinal disease. After implantation, these cells took root, though not enough of them did this to affect quality of vision. This study provides hope for the future development of regenerative treatments for patients with retinal degeneration [4]. Another group has demonstrated the therapeutic value of iPS cells by successfully treating a mouse model of sickle cell anemia with hematopoietic cells possessing a corrected version of the genetic defect [1]. IPS cells have also been used to treat a rat model of Parkinson's disease. Researchers transplanted iPS-derived dopamine neurons into the region of the rat brain that models the symptoms of the disease and observed subsequent improvement in the behavior of the rats receiving treatment [12]. In 2008, scientists generated iPS cells from patients with ten different diseases, including Duchenne muscular dystrophy, Down syndrome, juvenile diabetes mellitus, and Huntingdon disease. These results indicate a significant step toward using iPS cells to model diseases [6].

Due to their ability to differentiate into any cell type in the body, the use of iPS cells in medical research is very alluring. Though the technology to conduct clinical trials is still out of reach, researchers are already making strides to explore the potential medical uses of iPS cells, such as deriving iPS cells from the tissue of patients with genetic diseases and using the resultant cells to develop new disease models. This would be of particular benefit to researchers investigating diseases for which there is currently no true human model, like Parkinson's disease. The development of such models would also pave the way for the use of iPS cells in high-throughput screening of new drug treatments. A more distant goal, but perhaps the most attractive of all, is the use of iPS cells derived from a patient's own tissue in cell replacement therapy to treat damaged or nonfunctional tissues.

Today, iPS cells are a topic of great interest in research, and they promise to remain in the spotlight for years to come. Researchers and patients alike hope that this budding technology will eventually lead to better disease modeling, more efficient drug discovery, and perhaps someday the development of patient-specific cell replacement therapy for previously untreatable diseases.

References

[1] Hanna J, Wernig M, Markoulaki S, Sun C, Meissner A, Cassady JP, Beard C, Brambrink T, Wu L, Townes TM & Jaenisch R. (2007). Treatment of Sickle Cell Anemia Mouse Model with iPS Cells Generated from Autologous Skin. Science, 318:1920-1923.

[2] Kim D, Kim CH, Moon JI, Chung YG, Chang MY, Han BS, Ko S, Yang E, Cha KY, Lanza R & Kim KS. (2009). Generation of Human Induced Pluripotent Stem Cells by Direct Delivery of Reprogramming Proteins. Cell Stem Cell, 4(6):472-476.

[3] Kiskinis E & Eggan K. (2010). Progress toward the clinical application of patient-specific pluripotent stem cells. J. Clin. Invest., 120(1):51-59.

[4] Lamba DA, McUsic A, Hirata RK, Wang P, Russell D & Reh TA. (2010). Generation, Purification and Transplantation of Photoreceptors Derived from Human Induced Pluripotent Stem Cells. PLoS ONE, 5(1):e8763.doi:10.1371/journal.pone.0008763

[5] Okita K, Nakagawa M, Hyenjong H, Ichisaka T & Yamanaka S. (2008). Generation of Mouse Induced Pluripotent Stem Cells Without Viral Vectors. Science, 322(5903):949-953.

[6] Park IH, Arora N, Huo H, Maherali N, Ahfeldt T, Shimamura A, Lensch MW, Cowan C, Hochedlinger K & Daley GQ. (2008). Disease-specific induced pluripotent stem cells. Cell, 134(5):877-886.

[7] Soldner F, Hockemeyer D, Beard C, Gao Q, Bell GW, Cook EG, Hargus G, Blak A, Cooper O, Mitalipova M, Isacson O & Jaenisch R. (2009). Parkinson's Disease Patient-Derived Induced Pluripotent Stem Cells Free of Viral Reprogramming Factors. Cell, 136:964-977.

[8] Stem Cell Basics . In *Stem Cell Information* [World Wide Web site]. Bethesda, MD: National Institutes of Health, U.S. Department of Health and Human Services, 2009. Accessed February 13, 2010 at: http://stemcells.nih.gov/info/basics/defaultpage.

[9] Takahashi K & Yamanaka S. (2006). Induction of Pluripotent Stem Cells from Mouse Embryonic and Adult Fibroblast Cultures by Defined Factors. Cell, 126(4):663-676.

[10] Takahashi K, Tanabe K, Ohnuki M, Narita M, Ichisaka T, Tomoda K & Yamanaka S. (2007). Induction of Plurupotent Stem Cells from Adult Human Fibroblasts by Defined Factors. Cell, 131:1-12.

[11] Wernig M, Meissner A, Foreman R, Brambrink T, Ku M, Hochedlinger K, Bernstein BE & Jaenisch R. (2007). In vitro reprogramming of fibroblasts into a pluripotent ES-cell-like state. Nature, 448:318-324.

[12] Wernig M, Zhao J, Pruszak J, Hedlund E, Fu D, Soldner F, Broccoli V, Constantine-Paton M, Isacson O & Jaenisch R. (2008). Neurons derived from reprogrammed fibroblasts functionally integrate into the fetal brain and improve symptoms of rats with Parkinson's disease. PNAS, 105(15).

[13] Woltjen K, Michael IP, Mohseni P, Desai R, Mileikovsky M, Hämäläinen R, Cowling R, Wang W, Liu P, Gertsenstein M, Kaji K, Sung HK & Nagy A. (2009). PiggyBac transposition reprograms fibroblasts to induced pluripotent stem cells. Nature, 458:766–770

[14] Zhao X, Li W, Lv Z, Liu L, Tong M, Hai T, Hao J, Guo C, Ma Q, Wang L, Zeng F & Zhou Q. (2009). iPS cells produce viable mice through tetraploid complementation. Nature, 461:86-90.

Paige Dexter is a sophomore from Enterprise, Alabama, majoring in biology. She is currently conducting research with Dr. Guy Caldwell, studying Parkinson's disease in the Department of Biological Sciences. Though this review does not directly relate to her work, she wants to use this publication as a way to raise awareness about the stem cell research field. Paige is a National Merit Scholar and a Parkinson's Association of Alabama Scholar. She is the secretary for the Tri-Beta Biological Honor Society, a member of the Golden Key Honor Society, and a volunteer for the Humane Society of West Alabama.

Concussions in Sports: Diagnosis, Treatment, Management, and Perception

Connor Johnson
Faculty Sponsor: Jacqueline Morgan, Ph.D.

Department of Biological Sciences, University of Alabama, Tuscaloosa, AL 35487, USA

Concussions and head injuries are profound facets of sports and are complicated pathophysiological processes affecting the brain, caused by a traumatic force. Concussions typically involve short-lived impairment of neurologic function and a graded set of clinical symptoms. Diagnosis is difficult because of complexity and usually requires a multidimensional approach. Management of a concussion requires a gradual, multistep process, involving baseline testing, postural stability testing, and neurocognitive examination. Recent research has given some insight into the long term damage of brain trauma in sports and has placed concussions in the forefront of the public's perception. Young athletes as well as athletes with prior history of concussions are at a higher risk for postconcussional syndrome. Research advancements and increased awareness suggest promise for the coming decade in concussion research, prevention, and diagnosis.

Introduction

Postconcussional syndrome is a potential danger of sports and physical activity in general. The gravity of concussions; however, is often severely underestimated. Andre Waters, a football player who suffered multiple concussions, developed severe depression, and committed suicide, is a testament to the true severity of postconcussional syndrome [11]. There are approximately 300,000 reported concussions in the United States that occur while playing sports [19]. The diagnosis and treatment of this condition are subjects of controversy. A basic definition of postconcussional syndrome is a condition that results from a head injury and is characterized by central nervous system problems in the realms of somatic, psychological, and cognitive function [8]. Concussions result from a blow to the head that produces a cascade of neurological events. Following biomechanical injury to the brain, neurotransmitter release and ionic fluctuations result in ionic shifts and increased sodium-potassium pump activity [5]. This excessive activity requires large amounts of adenosine triphosphate (ATP), in which reduced blood flow to the brain creates an inequality between energy requirement and availability for the brain [12]. This lack of energy is one possible mechanism for increased susceptibility following concussion, as the brain is less able to respond to another injury [5]. Subsequently, a time of decreased glucose production occurs, which can last up to one month [12]. Increases in calcium can further aggravate the energy crisis and damage posttraumatic neural connectivity [5].

Diagnosis

Diagnosis for postconcussional syndrome can be difficult, as many of the symptoms are psychological or subjective. Clinical diagnosis consists of identifying the patient's history of traumatic brain injury and three or more of the following symptoms: headache, dizziness, fatigue, irritability, insomnia, concentration, memory difficulty, and intolerance of stress, alcohol, or emotion [1]. For athletes, on-field assessment involves examination of airway, circulation, neurologic performance, and the ability to perform simple tasks [3]. Previously, concussions were graded on scaling systems [3, 10]. Recently, however, these grading scales have been abandoned [3]. Most concussions (80-90 %) are resolved in seven to ten days, although this period can be longer in children and adolescents [14]. More severe concussions have prolonged or advanced symptoms and often are the result of multiple head insults [3]. The complicated nature of concussions and brain injury, in general, require a coordinated, multifaceted approach to diagnose [18]. The sports concussion assessment tool (SCAT) is the standard use for physician evaluation of a traumatic brain injury and involves symptom assessment, memory testing, and neurological performance testing [13]. Moreover, several computer programs exist to test neurocognitive function of patients [10].

Interestingly, magnetic resonance imaging has been utilized to detect prefrontal dysfunction following mild brain trauma in postconcussional syndrome patients. This could become an important tool for diagnostic purposes in the future [4].

Treatment and Management

Concussions are difficult to manage due to the complexity and relative lack of understanding of the injury. Most authorities recommend resting until all symptoms disappear and then using a graded program to return to full activity [2]. This progression begins with light exercise without resistance training, such as stationary biking and walking. The patient then moves to sport-specific exercises, while slowly adding resistance training. This is followed by non-contact drills, then full-contact practice after medical clearance, and concludes with full return [2]. Complex concussions, however, are more challenging to properly manage and may require neuropsychologic and postural stability testing, as well as a team of physicians to fully assess progression. It is essential that the individual wait until all symptoms are gone before returning to full activity, the individual is not left alone, and one day of rest occurs between each step in the progression [2]. Research also indicates that an individual with a history of a concussion is more likely to sustain another [8]. The period of rest immediately following the concussion is crucial, since athletes engaging in higher levels of activity perform worse in neurocognitive testing [12]. Athletic teams have also begun utilizing baseline neurocognitive testing before an injury occurs as a means of comparison since return to baseline levels is a good indicator of recovery from concussion [7]. An athlete with a concussion should avoid prescription medications except for acetaminophen, avoid complete bed rest, and be awakened periodically throughout the night to monitor symptoms if the athlete suffered from loss of consciousness or amnesia [7]. Ultimately, the key to concussion management is precaution. The increasing level of sensitivity that athletic teams are demonstrating towards players is a major positive step in preventing severe long term injury.

Discussion

Though the frequency of severe symptoms, depression, and/or suicide as a result of a concussion is low, diagnosis and recognition are becoming more prominent, particularly in sports. Furthermore, knowledge of the long term impact of postconcussional syndrome is finally being elucidated. Public awareness of concussion severity has rapidly expanded. Professional sporting organizations, most notably the National Football League (NFL), have begun pushing for greater awareness, better utility of protective equipment, and conservative approaches for players in practices and games. The NFL has even recently requested that players donate their brains to science upon their deaths so that postconcussional syndrome can be more thoroughly studied [17]. Well-known author, Malcolm Gladwell, has taken awareness to a whole new level with his writings, which compared football to dog fighting. This has raised a concern that football will reach a point where anyone who plays professionally is at an unparalleled risk for mental deterioration, dementia, and suicide [6]. His point is well supported, as an exceptionally large percentage of football players (and boxers) have been documented through brain autopsy with chronic traumatic encephalopathy, a chronic neurological disorder that results from head trauma [16]. Chronic traumatic encephalopathy is similar to Alzheimer's disease pathologically, with extensive tau neurofibrillary tangles but no amyloid [16]. Some scientists have also raised the possibility that some presumed Alzheimer's cases are actually the result of progressive brain trauma [6]. It is likely that brain trauma is more widespread than research statistics demonstrate and that young athletes are at risk as well. As athletes continue to augment in terms of size and speed, the frequency and relevance of postconcussional syndrome and head trauma, in general, will grow. It is crucial that sports leagues and science focus on preventative measures and treatment options. It is unlikely that treatments for highly advanced postconcussional syndrome will arise in the short term, so preventative equipment and regulations will play the largest roles. Rule adjustments and equipment renovations have been implemented already. For the latter, research studies have demonstrated a decrease in the prevalence of severe brain injuries but not in concussions [9, 15].

However, the combination of growing public awareness and research advancements offer reason for optimism in the next decade.

Conclusion

With the frequency of diagnosed concussions rising, the significance and understanding of head injuries have never been greater. The complexity of concussions presents a challenge for researchers and physicians. All athletic teams, but especially those involving adolescents or children, should be particularly cautious with players returning from concussions and should work to develop a consistent player management philosophy that involves a multifaceted approach. Due to novel research and technological advancement, concussion diagnosis continues to improve. Hopefully, more effective concussion prevention equipment will soon follow. Concussions are a prominent feature of sports and physical activity. However, with greater awareness and preventative strategies, the frequency of advanced postconcussional syndrome, chronic traumatic encephalopathy, and other chronic brain traumas could decrease.

References

[1] Boake C, McCauley SR, Levin HS, Pedroza C, Contant CF, Song JX, Brown SA, Goodman H, Brundage SI & Diaz-Marchan PJ. (2005). Diagnostic criteria for postconcussional syndrome after mild to moderate traumatic brain injury. J. Neuropsychiatry Clin. Neurosci., 17:350-356.

[2] Carson J, Tator C, Johnston K, Kissick J, Pursell L & Hunt B. (2006). New guidelines for concussion management. Can. Fam. Physician, 52:756-757.

[3] Covassin T, Elbin R & Stiller-Ostrowski JL. (2009). Current sports-related concussion teaching and clinical practices of sports medicine professionals. J. Athl. Trainer, 44:400-444.

[4] Datta SGS, Pillai SV, Rao SL, Kovoor JME & Chandramouli BA. (2009). Post-concussion syndrome: Correlation of neuropsychological deficits, structural legions on magnetic resonance imaging and symptoms. Neurol. India, 57:594-598.

[5] Giza CC & Hovda DA. (2001). The Neurometabolic Cascade of Concussion. J. Athl. Trainer, 36:228-235.

[6] Gladwell M. (2009). How different are dog fighting and football? The New Yorker.

[7] Guskiewicz KM, Bruce SL, Cantu RC, Ferrara MS, Kelly JP, McCrea M, Putukian M & McLeod TCV. (2006). Research based recommendations on management of sports related concussion: summary of the National Athletic Trainers' Association position statement. Br. J. Sports Med., 40:6-10.

[8] Hall RC, Hall RC & Chapman MJ. (2005). Definition, diagnosis, and forensic implications of postconcussional syndrome. Psychosomatics, 46:195-202.

[9] Knapik JJ, Marshall SW, Lee RB, Darakjy SS, Jones SB, Mitchener TA, delaCruz GG & Jones BH. (2007). Mouthguards in sports activities: history, physical properties and injury prevention effectiveness. Sports Med., 37:117-144.

[10] Lew HL, Thomander D, Chew KTL & Bleiberg J. (2007). Review of sport-related concussion: Potential for application in military settings. J. Rehabil. Res. Dev., 44:963-974.

[11] MacMullan J. (2007). I Don't Want Anyone to End Up Like Me. The Boston Globe.

[12] Majerske CW, Mihalik JP, Ren D, Collins MW, Reddy CC, Lovell MR & Wagner AK. (2008). Concussion in sports: Postconcussive Activity Levels, Symptoms, and Neurocognitive Performance. J. Athl. Trainer, 43:265-274.

[13] McCrory P, Johnston K, Meeuwisse W, Aubry M, Cantu R, Dvorak J, Graf-Baumann T, Kelly J, Lovell M & Schamasch P. (2005). Summary and agreement statement of the 2nd International Conference on Concussion in Sport, Prague 2004. Br. J. Sports Med., 39:196-204.

[14] McCrory P, Meeuwisse W, Johnston K, Dvorak J, Aubry M, Molloy M & Cantu R. (2008). Consensus statement on concussion in sport: the 3rd International Conference on Concussion in Sport held in Zurich, November 2008. J. Athl. Trainer, 44:438-448.

[15] McIntosh AS & McCrory P. (2005). Preventing head and neck injury. Br. J. Sports Med., 39:314-318.

[16] McKee AC, Cantu RC & Stern RA. (2009). Chronic traumatic encephalopathy in athletes: progressive tauopathy after repetitive head injury. J. Neuropathol. Exp. Neurol., 68:709-735.

[17] National Football League (2010). NFL reveals development in efforts to research head-trauma effects. www.nfl.com.

[18] Riggio S & Wong M. (2009). Neurobehavioral sequelae of traumatic brain injury. Mt. Sinai J. Med., 76:163-172.

[19] Theye F & Mueller KA. (2004). "Heads up": concussions in high school sports. Clin. Med. Res., 2:165-171.

Connor Johnson is a junior from Cullman, Alabama, majoring in biology with minors in English and Computer-Based Honors. He is currently working on a research project through the Computer- Based Honors Program with Dr. Karen Burgess, and he has previously worked with Dr. Stevan Marcus in the Department of Biological Sciences. He has been recognized by winning the Computer-Based Honors Freshman of the Year and Sophomore of the Year. He is also a mentor in the Big Brother Big Sister Program.

A Historical Perspective on the Role of Genomics in the Development and Utilization of Biological Weapons

Major B. Burch
Faculty Sponsor: Kim A. Caldwell, Ph.D.

Department of Biological Sciences, University of Alabama, Tuscaloosa, AL 35487, USA

Emerging sciences have the ability to widen the breadth of knowledge with which scientists are able to approach societal problems. However, certain realms of new intelligence may present challenges in a world where national security has become a major facet of international relations. Genomics, the study of the entire genetic sequence of individual organisms, is a developing subject within the biological sciences community. Progress made through advances in genomic science has allowed for greater complexity in the development of biological weapons. Designer pathogens created to take advantage of weaknesses in the human immune system are now possible. With increased governmental interests in the biodefense industry, it is important to consider how the scientific community is responding. It is likely that the future of this industry and policies related to biological weapons will develop in concert with advancements in the field of genomics.

Genomics as an Emerging Science

Genomics is the study of an organism's complete DNA sequence and is an emerging subject within the biological sciences community, made possible in part by the advancement of DNA sequencing technologies. In 2001, the human genome was sequenced in its entirety for the first time, offering insight into the many unknown aspects of our genetic history [2]. Since then, researchers have compiled the full genetic sequences of many other organisms. Because of the relative simplicity of their DNA sequences, many microorganisms represent the vast majority of our understanding of genetic mechanisms [2].

Technological advances have given humans an upper hand against dangerous pathogens, but science is quickly discovering that such technologies are also capable of enabling the creation of microbial generations that carry resistance to our defensive tactics [8]. Humans have been able to utilize various microbes to our advantage, but we may be approaching the point where our intentions overstep our knowledge. New tactics on the battlefield have shifted the war against microbes into one against humans [2,3]. With the science of genomics progressing at a rapid pace, the idea of genetically altering microbes for warfare purposes is becoming more prevalent, better understood, and increasingly threatening [2,5,7].

The pace at which the field of genomics is developing has been limited only by the creativity of the researchers involved. Advancements in sequencing tactics and data mining have lead to progressively more knowledge of the impacts of genetic alterations on disease phenotypes and transmission [2]. In recent years, genetic sequencing and recombination techniques have improved dramatically. The ease of genetic manipulation has made possible a new threat: designer microbes with possible malevolent intent [2].

The advancement of genomics has been possible due to easier access to gene databases, where entire genome codes for hundreds of different types of viruses and bacteria are stored [6]. The use of antibacterial soaps and hand sanitizer can influence the evolution of pathogens [8].The superbug is used to describe microbes that have been quickly evolving to adapt to our ways of life. The rapid adaptability and ease of genetic recombination have led scientists to explore the idea of utilizing microbes for human benefit, mostly on the level of fighting disease [2].

Genomics has led to one example of this idea, which used a smallpox vaccine in order to produce a possible vaccine for HIV [8]. Genetic material from inhibited HIV was placed into the stable and safe cowpox virus. This was made possible by the knowledge obtained from the full sequencing of the entire genomes of several strains of the smallpox virus [8]. Such a depth of genetic information has

given scientists important insight into the mechanisms and potential positive uses of these viruses [2,8].

However, once genetics began to be used widely throughout the field of microbiology, scientists began to reflect on possible threatening, pathogen hybrids [1,2,8]. Consider one early experiment where a scientist at Stanford University was able to transfer a dangerous gene from a virulent bacterial strain, related to the plague, into the harmless digestive microfloral bacteria *Escherichia coli*, creating a superbug that attacked human cells [8]. This emerging idea of novel biology was quickly sought by militaries around the world, thus leading to various proposals of designer pathogens whose harmful nature could possibly be harnessed in a laboratory and deployed on the battlefield.

Genetic Manipulation and the Development of Biological Weapons: Novel Biology

The evolution of biological warfare has taken place over an extensive period of time. Tactics such as the Mongols hurling the bodies of plague victims over the walls of besieged cities demonstrates an early example of biological warfare [5]. Other primitive examples include the distribution of smallpox-infested blankets to Native Americans by British colonists, and the use of biologically derived toxins on the tips of arrowheads throughout South America [5]. These tactics utilized the natural pathogenic properties of certain microorganisms to inflict harm on enemy populations. In the mid 1970s, genetic engineering made its way into the realm of novel bioweaponry shortly after the discovery of the helical structure of DNA [1,5]. Manipulation of the blueprints of life allowed scientists and the military to alter the functions of dangerous biological agents. Open criticism to military research using genetically altered microorganisms quickly rose from the civilian academic community. In the mid 1980s, Charles Piller and Keith Yamamoto obtained documents describing the history of United States biological weapons research. They revealed that the use of biotechnologies for offensive military purposes was unlikely because of the complex nature of large-scale biological research [5]. However, individuals within the intelligence community speculated that the Soviet Union was performing research on exotic biological agents. Further investigation revealed that both the United States and the Soviet Union were collecting samples of Ebola and Marburg viruses in Africa, two microbes that cause intense cases of hemorrhagic fever. Both sides were conducting bioweapons research of an offensive nature [1,5].

Reports later revealed that during this time the Soviet Union's biological weapons directorate, Biopreparat, commissioned thousands of scientists to study the most efficient and effective forms of production and application of pathogenic microbes on the battlefield [1,5]. Along with the mass production of biological weapons, Biopreparat was heavily engaged in the genetic alteration and combination of many different pathogens. In one instance, its scientists transferred genes from cobras into otherwise harmless bacteria and viruses [1]. The goal of this procedure was to create bacterial cells that could multiply and produce deadly venom in a victim's body. Examples of this nature demonstrate the lengths to which governments were attempting to use genetic science for military advantage.

In 1995, a survivalist named Larry Harris from Ohio purchased three vials of plague bacteria from the American Type Culture Collection [5]. Although Harris claimed his intentions were only to produce his own antidote to the microbes, this action sent a clear message that America's laws lacked the ability to ensure safety from domestic biological threats [5]. This incident also underscored the ease with which amateur scientists could potentially alter and weaponize pathogens in the privacy of their own homes or personal laboratories. In response, domestic restrictions concerning the procurement and handling of sensitive biological agents tighten in 1996. Harris's disturbing actions initiated a period of research and public safety exercises to improve the ability of first responders to assess and mitigate the hazards of a domestic biological attack [5].

As the new millennium approached, public health and national security experts made recommendations to stockpile vaccines for agents such as anthrax [5]. At this time, the House Committee on Government Reform concluded from their investigation that techniques such as gene splicing could produce vaccine-resistant strains of viruses. This raised the concern that the U.S. vaccine program only offered a limited form of defense

against possible biological assaults [5]. Thus, the genetic engineering of weaponized pathogens ushered in a new era for biosecurity and created an evolving challenge for national security officials.

Genomics and United States Biodefense Research

A recent example of the importance of genomic studies in biological warfare came after the terrorist attacks of September 11, 2001. Envelopes filled with highly refined *Bacillus anthracis* spores, an agent causing anthrax, were sent to several prominent U.S. senators and members of the media [3]. It was revealed that the *B. anthracis* used in the attack was genetically identical to strains of the bacteria kept in research laboratories at the Centers for Disease Control and Prevention (CDC) and the United States Army Medical Research Institute of Infectious Diseases (USAMRIID) [3]. The strain of bacteria used in the attack was studied, and its whole genome sequence was compared with those of known strains. Scientists concluded that minor mutations in the strains used in the attack were descended from those held in the government laboratories [3]. By previously sequencing the entire genomes of known *B. anthracis*, the investigators were able to arrive at their conclusion quickly. The genetic studies indicated that someone within the U.S. scientific community was responsible for the attacks [3].

The development of biological weapons is a growing concern because (i) they are relatively easy to manufacture on a small scale, and (ii) microbial genome databases are expanding, as well as the scientific literature, which now provide information regarding all potential genes involved in pathogenicity and virulence, colonization of host cells, immune response evasion, and antibiotic resistance [2].

Although the publically available data on genomics research may be subject to malicious intent, it also has the ability to provide treatments and vaccines for weaponized biological agents [2]. This concept is already being utilized, in that sequencing the entire human genomes, as well as the genomes of common human pathogens, is offering insight into particular infectious disease processes. By using DNA microarrays and proteomics analyses, scientists can demonstrate the step-by-step events that take place within human cells during an infection by a particular pathogen [2]. From this knowledge, drugs and vaccines may be produced to help alleviate or defend against potential biological attacks. For instance, while developing rapid detection techniques to be used in bioweapon sensors, researchers used comparative genome hybridization to discover strain-specific traits of virulence and antigenicity within *Helicobacter pylori* and *Streptococcus pneumoniae*, both of which are common human pathogens [2]. Increases in federally funded grants for biodefense have reinforced the discovery of general knowledge regarding typical disease processes [7].

However, increases in federal funding have been due, largely, to the increased risks of domestic attacks using weaponized biological agents [7]. Research concerning the mitigation or prevention of illnesses caused by a biological attack has been of great interest to the United States government. Following the attacks of 9/11, there was a new political emphasis on funding research related to national security [4,7]. Biodefense began as a relatively small sector of the national security framework, but it saw a tremendous rise in funding in the ensuing years (Figures 1 and 2) [4].

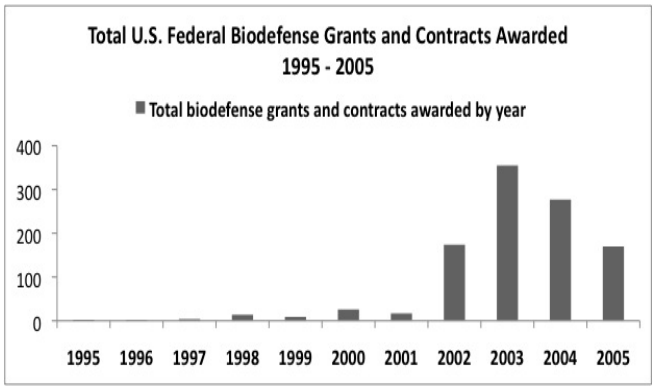

Figure 1. Total number of grants awarded by the U.S. government to public and private firms for the pursuit of research regarding mitigation and prevention of possible biological attacks [4].

The increased cost of research for mitigating biological weapons reflects the vast technical improvements that have been made towards methods to identify genetic variations that may make certain pathogens useful as biological weapons [4]. Research ventures in direct biodefense reflect high-cost, high-reward investment opportunities for firms

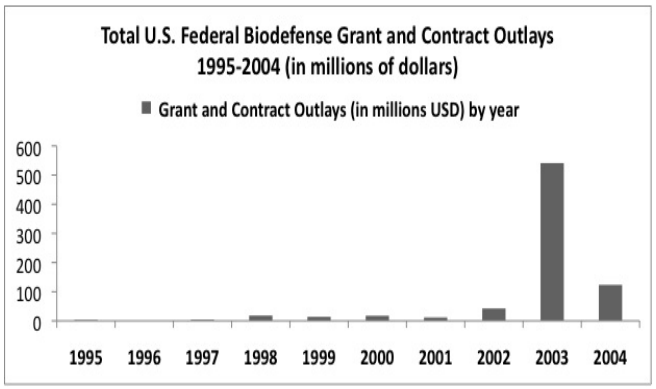

Figure 2. Total outlay amounts (in millions of U.S. dollars) of grants awarded by the U.S. government to public and private firms for the pursuit of research regarding mitigation and prevention of possible biological attacks [4].

in this sector. Their successes are subsidized by government funds, while their failures to develop useful commodities prove to be substantially costly to investors in the long run [4].

Although the American biodefense industry is still in its emerging stages, it has proven to be extremely profitable for private investors in the short-tem [4]. With research enterprises commissioned by major pharmaceutical companies and small laboratory groups alike, there is great diversity among American biodefense firms. It should also be noted

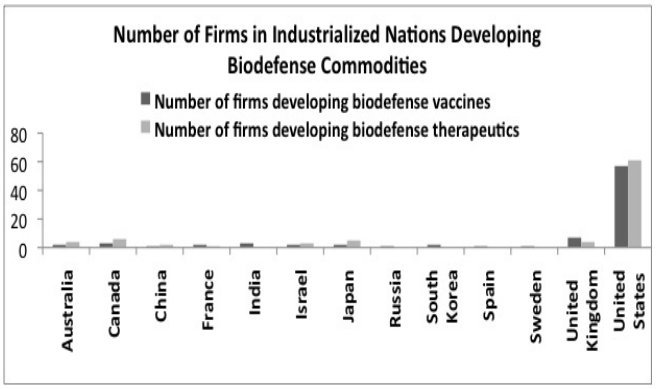

Figure 3. Number of private firms within industrialized nations pursuing the development of vaccines and therapeutics in response to possible biological attacks [7].

that the United States is home to the largest number of enterprises dedicated to biodefense research (Figure 3) [7]. This fact is true for both the development of vaccines and therapeutics.

Conclusion

Biodefense remains a very complex issue for the academic community to analyze, as many facets of America's biodefense and biosecurity programs are not available for public review. The federal government justifies this secrecy due to the involvement of sensitive national security data. Additionally, private industries also regard many of the aspects involved as trade secrets. Beyond the scope of national security, advances in genomic science will continue to provide the biological sciences community with new tools to analyze and understand microbial life cycles. Although these advances will likely correspond to security hazards for our nation, it is also likely that these same advances will offer researchers the tools to diminish the effects of biological hazards. This situation demonstrates increasing complexity in the development of biological weapons, but a future in which the impact of those weapons may be minimized. The study of genomes represents a new frontier in the biological sciences community, offering insight both into our shared history and our looming future. Society has recognized that a right to knowledge is essential, especially within the review processes of groundbreaking research. However, we must also be stewards of this knowledge. The evolution of microbes is occurring, both by natural and human-influenced means. Society must strive to ensure that noble intentions regarding the outcomes of genomic research will prevail over those of individuals with malicious objectives.

References:

[1] Alibek K. (1999). Biohazard: The Chilling True Story of the Largest Covert Biological Weapons Program in the World - Told from the Inside by the Man Who Ran It. New York, NY: Random House.

[2] Fraser CM & Dando MR. (2001). Genomics and future biological weapons: the need for preventive action by the biomedical community. Nature Genetics, 29:253-256.

[3] Leitenberg M. (2002). Biological Weapons and Bioterrorism in the First Years of the Twenty-First Century. Politics and the Life Sciences, 21:3-27.

[4] Lentzos F. (2007). The American biodefense industry. Politics and the Life Sciences, 26:15-23.

[5] Miller J, Engelberg S & Broad W. (2002). Germs: Biological Weapons and America's Secret War. New York, NY: Simon and Schuster.

[6] Ryan F. (1997). Virus X: Tracking the New Killer Plagues. New York, NY: Little, Brown and Co.

[7] Trull MC, du Laney TV & Dibner MD. (2007). Turning biodefense dollars into products. Nature Biotechnology, 25:179-184.

[8] Zimmerman BE & Zimmerman DJ. (2003). Killer Germs: Microbes and Diseases that Threaten Humanity. New York, NY: McGraw-Hill.

Major Benjamin Burch is a senior from Birmingham, Alabama, with majors in biology and economics and a minor in the Blount Undergraduate Initiative. He conducts research with Dr. Margaret Johnson in the Department of Biological Sciences, using biochemical and molecular analyses to study the genetic regulation of inostiol phosphate biosynthesis. Major is a Presidential Scholar and the recipient of the 2009 Outstanding Undergraduate Award in the Department of Economics. Beyond his work in the lab, he is also a Blackburn Institute Fellow and the President of Sustained Dialogue.

2011 Submission Guidelines

We accept articles from current undergraduate students at The University of Alabama (UA). If you are a graduate student or recent alumni of UA, we will consider your article if the majority of your work was conducted while you were an undergraduate at UA. Undergraduate students from other institutions may submit; however, priority will be given to those who conducted their research at UA through a summer or special program.

1. Your name, e-mail address, and phone number must be included.

2. Your submission must relate to science or health.

3. Your work must be sponsored by a faculty member.

4. The length of your submission must be between 1000 and 3500 words. We will accept a longer submission if the author can limit the submission to the required length for the publication, and any extra material is able to be published online.

5. Figures, charts, and graphs are allowed but not required. (Note: The color will be mostly black and white.)

6. Your paper must contain an abstract.

7. Your citations must follow the guidelines listed on our website at BAMA.UA.EDU/~JOSHUA.

8. The deadline for submission is February 7, 2011.

9. E-mail submissions to joshua.alabama@gmail.com

JOSHUA was made possible by the following organizations:

University of Alabama
Office of the Provost

Tri-Beta National Honor Society
Kappa Beta Chapter

Howard Hughes Medical Institute

National Science Foundation


THE UNIVERSITY OF ALABAMA
1831